



An-Najah National University
Faculty of Graduate Studies

***ZNO/BENTONITE COMPOSITE FOR
TETRACYCLINE REMOVAL FROM WATER VIA
ADSORPTION AND PHOTO-DEGRADATION***

By

Yasmeen Alaa Mohammad Hamdan

Supervisor

Prof. Ahed Zyoud

**This is Submitted in Partial Fulfillment of the Requirements for the Degree of Master of
Chemistry, Faculty of Graduate Studies, An-Najah National University, Nablus - Palestine.**

2025


ZNO/BENTONITE COMPOSITE FOR TETRACYCLINE REMOVAL FROM WATER VIA ADSORPTION AND PHOTO-DEGRADATION

By

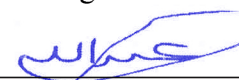
Yasmeen Alaa Mohammad Hamdan

This Thesis was Defended Successfully on 10/04/2025 and approved by

Prof. Ahed Zyoud
Supervisor


Signature

Dr. Abdullah Eid
External Examiner


Signature

Dr. Derar Al-smadi
Internal Examiner


Signature

Dedication

I dedicate this thesis to myself, in appreciation for every moment I worked hard, and every step I took toward achieving this accomplishment. I am now proud of myself and what I have achieved, and I ask God to make this the beginning of greater accomplishments.

I dedicate it to the people of Gaza, who suffer in silence but remain an example of steadfastness and resilience. In every word, in every step, I find my strength in you and realize that I resist with my knowledge, just as you resist with your sacrifices and your determination that does not know defeat.

I dedicate it to all those who care about the environment, to all those who love the earth and recognize its right to be preserved and cared for, and to all those who believe that every tree and every drop of water is a blessing that deserves to be preserved.

.

Acknowledgements

I would like to start by thanking myself, then myself, then myself. My ambition has always been the top, and this achievement is just the beginning of the road. The top is just the beginning of flying and setting off new horizons of excellence and creativity. I am proud of what I have achieved thus far, but I am certain that this is just the beginning of what is bigger and greater.

I would also like to thank my supervisor, Dr. Ahed Zyoud, who has been instrumental in guiding and directing me. Thanks to him, I have learned many academic and research skills that will remain entrenched in my future career. I also cannot forget to thank the distinguished laboratory technician, Ameen Amaira, who was a true partner in the success of this work. He contributed to helping me overcome all the practical difficulties I faced. He was always ready to help me at any time.

I would also like to extend my sincere thanks and gratitude to my friends (Ms. Sahar and Ms. Nadeen) and family, who have been my greatest support at every moment. I would also like to thank all the unknown soldiers who have been the reason for giving me strength and supporting me in times of need. Their presence in my life was like a balm that alleviated every difficulty and gave me hope in every step.

I thank you all from the bottom of my heart. You are all part of this success, and every word of gratitude is not enough to express my appreciation and gratitude to you. However, nothing is equal to thanking myself first. Every step, every moment, and every challenge was caused by my insistence and determination to be the best. I am proud of myself; my pride reaches the sky because I am always at the top. I almost feel that I now need a Nobel Prize for my efforts!

In conclusion, O Allah, use us and do not replace us, benefit us and benefit others through us, close the gaps of your nation with us and protect us from the evil of hypocrisy and keep away from us indolence and laziness, O Allah, grant us the light of the mind and purity of the heart, and reward us with what you are worthy of, and make us among those who listen to the word and follow the best of it. O Allah, make our deeds pure for your sake, and guide us to what you love and are pleased with.

Declaration

I, the undersigned, declare that I submitted the thesis entitled:

ZNO/BENTONITE COMPOSITE FOR TETRACYCLINE REMOVAL FROM WATER VIA ADSORPTION AND PHOTO-DEGRADATION

I declare that the work provided in this thesis, unless otherwise referenced, is the researcher's own work, and has not been submitted elsewhere for any other degree or qualification.

Student's Name: Yasmeen Alaa Mohammad Hamdan

Signature:



Date:

2025/04/10

List of Contents

Dedication	III
Acknowledgements	IV
Declaration	V
List of Contents.....	VI
List of Tables	IX
List of Figures	X
List of Appendices	XI
Abstract.....	XIII
Chapter One: Introduction.....	1
1.1 Background.....	1
1.2 Sources of water pollution	2
1.2.1 Pharmaceutical residues.....	3
1.2.1.1 Tetracycline	4
1.3 Water treatment techniques	6
1.3.1 Adsorption technique	8
1.3.1.1 Adsorbent materials	9
1.3.2 Photodegradation	12
1.3.2.1 Photocatalysis	13
1.4 Aims of the study	16
Chapter Two: Experimental.....	17
2.1 Materials and Instruments.....	17
2.1.1 Chemicals.....	17
2.1.2 Equipment.....	17
2.1 Preparation of Solutions.....	18
2.1.1 Stock solution	18
2.1.2 Other solutions required.....	18
2.2 Preparation of the ZnO/bentonite composite catalyst.....	18
2.3 Photo-catalytic system and parameter effects.....	19
2.3.1 Photo-catalytic system	19
2.3.2 Effect of catalyst amount	19
2.3.3 Effect of initial tetracycline concentration.....	19
2.3.4 Effect of pH	20

2.3.5 Effect of temperature	20
2.3.6 Effect of oxygen.....	20
2.3.7 Effect of carbon dioxide	20
2.3.8 Recovery of the catalyst and reuse	20
2.3.9 Complete mineralization.....	21
2.4 Control experiments.....	21
2.4.1 In the absence of a catalyst	21
2.4.2 In the dark	21
2.4.3 In light.....	22
2.5 Zero-point charge.....	22
Chapter Three: Results and discussion	23
3.1 Characterization results.....	23
3.1.1 UV–Vis	23
3.1.2 X-ray diffraction (XRD) patterns	24
3.1.3 Energy dispersive X-ray (EDX)	28
3.1.4 Scanning electron microscope (SEM)	30
3.1.5 Zero-point charge - ZPC	31
3.2 Tetracycline photodegradation study.....	32
3.2.1 Control experiment results.....	33
3.2.2 pH effect	35
3.2.3 Temperature effect.....	37
3.2.4 Effect of the amount of ZnO/bentonite catalyst.....	39
3.2.5 Effect of the tetracycline concentration	40
3.2.6 Effect of oxygen.....	41
3.2.6 Effect of carbon dioxide	42
3.3 Kinetics of tetracycline photodegradation	43
3.4 Activation energy.....	47
3.5 Order of the reaction	48
3.6 Recovery and reuse of the ZnO/bentonite catalyst	50
3.7 Tetracycline complete mineralization confirmation	50
38 Conclusion	53
3.9 Recommendations for future work	54
List of Abbreviations	56
References.....	57

Appendices.....	68
الملخص.....	ب

List of Tables

Table 1.1: Tetracycline specifications.....	5
Table 3.1: Effects of the TC concentration and catalyst amount on the kinetic parameters of photodegradation.....	45
Table 3.2: Effects of temperature and pH on the kinetic parameters of photodegradation.....	46
Table 3.3: Effects of oxygen and carbon dioxide on the kinetic parameters of photodegradation.....	46
Table 3.4: Confirmation of complete mineralization of tetracycline by ZnO/bentonite-catalyzed photodegradation. The reaction was conducted with TC (100.0 mL, 40 ppm) and 0.1 g of ZnO/bentonite at pH ~8.5 at 25 °C.	51

List of Figures

Figure 1.1: Semiconductor after irradiation with light in the photocatalysis reaction	14
Figure 3.1: Solid-state electronic absorption spectra measured for ZnO powder, bentonite and ZnO/bentonite. Measurements were performed using a tetracycline solution (40 ppm, 100 ml) with 0.1 g of the catalyst. Baseline correction was made with distilled water.	24
Figure 3.2: X-ray diffraction pattern of the ZnO powder.	25
Figure 3.3: X-ray diffraction pattern of bentonite clay.	26
Figure 3.4: X-ray diffraction pattern of the ZnO/bentonite composite.	27
Figure 3.5: Shows the X-ray spectrum of a raw bentonite clay sample, with prominent peaks representing the different elements in the sample. The accompanying table shows the percentages of the atomic composition of the elements detected in the sample.	28
Figure 3.6: Shows the X-ray spectrum of a ZnO/bentonite composite sample, with prominent peaks representing the different elements in the sample. The accompanying table shows the percentages of the atomic composition of the elements detected in the sample.	29
Figure 3.7: SEM image of the bentonite microflacks.	30
Figure 3.8: SEM image of ZnO/bentonite.	31
Figure 3.9: Plots of ΔpH vs. initial pH measured for ZnO, bentonite clay, and ZnO/bentonite clay. The experiment was performed at 25 °C. Intercepts show values of pH_{pzc} for different solids.	32

List of Appendices

Appendix A: Figures.....	68
Figure A.1: Basic structures of clay minerals: a) Octahedral sheets and b) tetrahedral sheets.	68
Figure A.2: Structures of a) 1:1 and b) 2:1 clay minerals.....	68
Figure A.3: Structure of expandable and nonexpandable 2:1 clay minerals.....	69
Figure A.4: Basic structure of bentonite clay.	69
Figure A.5: Absorption spectra of the tetracycline solution in distilled water at neutral pH at room temperature.	70
Figure A.6: Absorption spectra of the photodegradation of tetracycline in the presence of a ZnO/bentonite photocatalyst. The experiment was performed using a tetracycline solution (100 ml, 40 ppm) at 25 °C and basic pH medium with 0.1 g of ZnO/bentonite under simulated solar light.	70
Figure A.7: Effects of light on tetracycline removal: Comparison of the photodegradation reactions of tetracycline alone and with three different catalysts (ZnO, bentonite, and ZnO/bentonite) over time (initial concentration of 40 ppm, temperature of 25 °C and 0.1 g of each catalyst).	71
Figure A.8: Effects of the absence of light on tetracycline removal: Comparison of the effects of three different catalysts (ZnO, bentonite, and ZnO/bentonite) on the photodegradation of tetracycline with time (initial concentration of 40 ppm, temperature of 25 °C and 0.1 g of each catalyst).	71
Figure A.9: The chemical structure of a tetracycline molecule, with pK _a values for the main functional groups: pK _{a1} = 3.3, pK _{a2} = 7.7, and pK _{a3} = 9.7, indicating the dissociation and ionization points of the compound when the pH changes.....	72
Figure A.10: Different ionic forms of tetracycline (TCH ₃ ⁺ , TCH ₂ , TCH ⁻ , TC ²⁻) at different pH values	72
Figure A.11: Effect of different pH values (3.0, 5.3, 7.0, 8.5, 10.1) on the percentage of tetracycline removal of tetracycline over time, with initial concentration of 40 ppm, temperature set at 25°C, and 0.1 g of ZnO/bentonaite catalyst.	73
Figure A.12: Effect of different temperatures values (7°C, 15°C, 30°C, 57°C) on the percentage of tetracycline removal of tetracycline over time, with initial concentration of 40 ppm, basic pH medium, and 0.1 g of ZnO/bentonaite catalyst.	73
Figure A.13: Effect of different catalyst amounts (0.05 g, 0.1 g, 0.2 g, 0.3 g, 0.4 g, 0.5 g) on the percentage of tetracycline removal over time, with an initial concentration of 40 ppm, basic pH medium, and temperature set at 25°C.	74
Figure A.14: Effects of different tetracycline concentrations (10 ppm, 20 ppm, 30 ppm, 40	

ppm, and 50 ppm) on the percentage and amount of tetracycline removed over time, with 0.1 g of ZnO/bentonite catalyst, basic pH medium, and temperature set at 25 °C. The red curve represents the percentage removal of tetracycline (left y-axis), whereas the blue curve represents the amount of tetracycline removed in mg/L (right y-axis)..... 74

Figure A.15: Effect of oxygen on the percentage of tetracycline removal over time, with an initial concentration of 40 ppm, 0.1 g of ZnO/bentonite catalyst, basic pH medium, and temperature set at 25 °C..... 75

Figure A.16: Effect of carbon dioxide on the percentage of tetracycline removal over time, with an initial concentration of 40 ppm, 0.1 g of ZnO/bentonite catalyst, basic pH medium, and temperature set at 25 °C..... 75

Figure A.17: Relationship between $\ln(k)$ and $\frac{1}{T}$ in the tetracycline removal reaction using the ZnO/bentonite catalyst, where the data follow a straight line with the regression equation ($y = -602.84x + 6.1598$)..... 76

Figure A.18: Relationship between $\ln(\text{rate})$ and $\ln([\text{tetracycline concentration}])$, with the straight-line equation $y = 0.21497x + 4.66428$ and a correlation coefficient $R^2 = 0.93135$ 76

Figure A.19: Relationship between $\ln(\text{Rate})$ and $\ln([\text{catalyst amount}])$, with the straight-line equation $y = 0.10224x + 4.1696$ and a correlation coefficient $R^2 = 0.91324$. . 77

Figure A.20: Photocatalytic efficiency of ZnO/bentonite after recovery and reuse. Experiments were performed using a tetracycline solution (100 mL, 40 ppm) with 0.1 g of catalyst at a temperature of 25 °C and pH 8.5..... 77

Figure A.21: Electronic absorption spectral confirmation of complete mineralization of tetracycline by photodegradation with time. The reaction was conducted with TC (100.0 mL, 40 ppm) and 0.1 g of ZnO/bentonite at pH ~8.5 at 25 °C. 78

Figure A.22: FT-IR spectra of tetracycline, with air utilized as the blank..... 78

Figure A.23: FT-IR spectra of the ZnO/bentonite catalyst, with air utilized as the blank. 79

Figure A.24: FT-IR spectra of tetracycline on the catalyst surface after 30 min of photodegradation. The reaction was performed with TC (100.0 mL, 40 ppm) and 0.1 g of ZnO/bentonite at pH ~8.5 at 25 °C. Air was used as the blank... 79

Figure A.25: FT-IR spectra of tetracycline on the catalyst surface after 90 min of photodegradation. The reaction was performed with TC (100.0 mL, 40 ppm) and 0.1 g of ZnO/bentonite at pH ~8.5 at 25 °C. Air was used as the blank... 80

Figure A.26: FT-IR spectra of tetracycline on the catalyst surface after 180 min of photodegradation. The reaction was performed with TC (100.0 mL, 40 ppm) and 0.1 g of ZnO/bentonite at pH ~8.5 at 25 °C. Air was used as the blank... 80

ZNO/BENTONITE COMPOSITE FOR TETRACYCLINE REMOVAL FROM WATER VIA ADSORPTION AND PHOTO- DEGRADATION

By

**Yasmeen Alaa Mohammad Hamdan
Supervisor**

Prof. Ahed Zyoud

Abstract

Water pollution by pharmaceuticals, especially tetracycline, is an urgent and rapidly expanding environmental issue, that exacerbated by increased drug use and improper disposal. This emphasizes the need for strategies and approaches to treat contaminated water in a manner that protects the environment and organisms from the negative effects of tetracycline residues.

The ZnO/bentonite composite demonstrates excellent adsorption capabilities due to the porous structure of bentonite clay, which offers a large surface area ideal for attracting and capturing pollutant particles. On the other hand, the composite exhibits remarkable efficiency in breaking down these pollutants by taking advantage of the photocatalytic properties of ZnO, where it serves as a highly effective photocatalyst under ultraviolet light, assisting in the decomposition of pollutants into less harmful components.

In this study, ZnO was supported on bentonite and utilized as a photocatalyst under simulated solar light. The research included studying the physical and chemical properties of the composite via various analytical methods. This study helps provide insights into the structure and composition of this catalyst and aids in understanding their effectiveness in pollutant treatment. In addition, a kinetic study was carried out to assess the efficiency of tetracycline removal and understand the reaction mechanism.

The performance of both the adsorption and photocatalysis of the ZnO/bentonite compounds in removing tetracycline from water was also evaluated under different conditions, such as pH, tetracycline concentration, temperature, amount of catalyst, and other factors, such as the effects of oxygen gas and CO₂ gas, where the composite achieved high degradation rates with remarkable efficiencies of up to 87%. In addition, nearly complete mineralization of up to 98% was achieved, confirming the ability of the catalyst to perform the complete degradation of the tetracycline antibiotic into nontoxic byproducts.

Additionally, the composite was reused while maintaining its good performance, making it a sustainable and effective solution for treating water pollution and protecting the environment.

Keywords: Water Pollution, Tetracycline, ZnO/Bentonite Composite, Photocatalyst, Adsorption, Photocatalysis, Complete Mineralization.

Chapter One

Introduction

1.1 Background

Water is the spirit that quenches the Earth's thirst and gives life to all that is living. Water is considered one of the most important natural resources that plays a decisive role not only in the continuity of life but also in preserving ecosystems and various human activities from agriculture to industry to trade, and in every aspect of our lives, water is indispensable.

Water covers approximately 71% of the planet's Earth [1], but unfortunately, the largest portion of this percentage is saltwater and ocean water; only 3% of this water is fresh water, and a large portion of it is still confined to rivers and ice caps, leaving less than 1% available for human use in rivers, lakes and groundwater [2]. As a result, fresh water is a limited and valuable resource, the preservation of which has become a collective responsibility to ensure the continuity of life.

However, access to safe and clean drinking water is a major challenge in many parts of the world despite its importance [3]. More than 40% of the world's population lacks access to clean water [4], this is attributable to the fact that most water resources are subject to large and escalating amounts of pollutants. Pollution is not only limited to agricultural and industrial wastes but also includes a wide range of chemical pollutants released into the aquatic environment, including dyes, heavy metals, and pharmaceutical residues [5]. These pollutants can leak into water supplies via industrial effluents or sewage [6], thus creating grave danger to human health and the environment. According to the World Health Organization, polluted water can spread diseases and lead to the death of approximately 3.4 million people every year [7]. With the escalation of population growth, industrialization and urban sprawl, the demand for water is increasing, thus intensifying pressure on water resources [8]. Therefore, the prevention of pollution and the need for efficient management strategies and techniques to remove pollutants have become increasingly important. To meet this challenge, existing water treatment technologies have progressed from traditional filtration techniques through electrolysis, nanotechnology, and biological treatment to adsorption and photodegradation [9].

As a result, scientists and researchers have worked on these technologies to make them effective, safe, low cost, applicable, and widely used under various conditions, and through all of this continuous work, scientists have been able to design more effective methods to treat polluted water, which in turn will help us maintain the environment and clean potable and safe water for human consumption.

1.2 Sources of water pollution

Water pollution is the process of introducing harmful substances into water, leading to their deterioration [10]. Water pollution occurs as a result of the exposure of rivers, lakes, and oceans to pollutants that in turn change the chemical, physical, or biological properties of the water [11], making it unsuitable for human or animal use or even for natural environmental activities.

These pollutants can be natural or artificial [12] and vary in composition and type among chemical, biological, and physical pollutants [13]. Chemical pollutants include toxic substances such as heavy metals, pesticides, industrial chemicals, and pharmaceutical residues [14], whereas biological pollutants include microorganisms such as bacteria and viruses [15], and physical pollutants include solid particles and impurities [16]. These pollutants deteriorate water quality and negatively affect organisms.

There are many sources of water pollution that vary according to the type of pollution and the causes that lead to it. Water pollution can result from human sources, which include all activities carried out by humans that lead to the introduction of pollutants into water sources, such as direct discharge of sewage and household waste into rivers, lakes without adequate treatment [17]; animal sources, which occur mainly through farms and pastures, such as the discharge of animal waste into rivers and lakes, which can cause water pollution with organic matter and bacteria [18]; and agricultural sources, which constitute a major source of water pollution through the use of chemical fertilizers and pesticides, which contain harmful chemicals that can drift with rainwater into water bodies, polluting the aquatic environment [19]; and finally, industrial sources, which are among the most prominent dangerous sources of pollution, as they include all industrial activities that release pollutants into water sources, including chemicals, toxic heavy metals such as mercury and lead, organic waste, and various drug residues [20]. In addition, industrial waste can contain nonbiodegradable materials, which can accumulate in the environment, causing serious effects on marine life and human health, including

chronic disease, poisoning, and widespread environmental damage [21].

Each of these types of sources contributes to water pollution in different ways, affects water quality, and threatens the lives of many living organisms. Understanding the sources of water pollution and their mechanisms is necessary to develop effective strategies for treating water and protecting it from pollution.

1.2.1 Pharmaceutical residues

Pharmaceuticals are considered essential and necessary for human and animal health, but they have been recognized as an environmental problem when their residues leak into fresh water sources [22]. In recent decades, water pollution with pharmaceutical residues has become an important environmental and health issue.

Pharmaceutical residues in water can be defined as industrial chemical compounds that are manufactured to be used as medicines, either with a prescription or as nonprescription treatments to treat various diseases that may affect humans, or they can be veterinary medicines used to treat diseases that affect animals [23]; among these drugs, antibiotics stand out, which are considered the most common and commonly used drugs and are among the main pollutants that have serious effects on the environment.

Antibiotics can enter water bodies and sources in several ways; one of the main ways is through sewage discharge. When humans or animals take antibiotics, a large portion of them are not absorbed by the body but are eliminated through urine or feces [24]. These wastes then enter sewage systems that may not be able to remove all of the drug compounds during traditional treatment processes. In addition, improper disposal of unused medications, whether by individuals, medical institutions, or even factories, can contribute significantly to water pollution [25], which in turn carries these compounds to eventually reach rivers, lakes, and groundwater, causing contamination.

Residues of antibiotics in water can have serious effects on various organisms in aquatic systems, as continuous exposure of aquatic organisms to low concentrations of antibiotics can lead to the development of bacteria resistant to these drugs in the environment [26]. These resistant bacteria, in turn, represent a major challenge because they reduce the effectiveness of antibiotics in treating human and animal diseases. It is estimated that infection with antibiotic-resistant bacteria caused the death of nearly 5 million people in 2019 [27], making it one of the 10 greatest public health threats facing humanity, according to the World Health Organization [28].

The residues of pharmaceutical preparations, especially antibiotics, represent a serious environmental challenge, especially since pharmaceutical preparations are designed to be stable or semistable to reach the target molecules and interact with them [29].

This means that they are difficult to decompose via traditional methods. The presence of 47 types of antibiotics, which are classified into four main categories, namely, macrolides, fluoroquinolones, sulfonamides, and tetracyclines, increases their survival in the environment [30].

The presence of antibiotics in water sources poses a threat to the environment and affects living organisms, so great efforts are needed to address their effects and develop technologies that work to eliminate them effectively and with high efficiency.

1.2.1.1 Tetracycline

Tetracycline (TC) is an antibiotic that falls into the antibiotic class called tetracyclines. This antibiotic has become famous for eliminating many strains of harmful bacteria. Many diseases and bacterial infections, such as cholera, syphilis, plague, acne, malaria, urinary tract infections, skin infections, respiratory infections, etc., etc., affect people [31]. Tetracycline is also widely used in veterinary medicine to treat and prevent animal bacterial infections [32].

The TC story began in the 1940s, when "Benjamin Dugard," an American chemist, first discovered "chlortetracycline" compounds from this class [33]. In 1948, this compound was found in a soil sample that contained the bacteria "Streptomyces aureus", the source of TC [34]. During the 1950s, the pure form of TC was subsequently found, where large quantities were produced as excellent antibiotics against many diseases [35].

Its name comes from its unique structure. There are four linked carbon rings called the tetracycline ring system ($C_{22}H_{24}N_2O_8$) [36]. These rings are arranged so that the molecule has a nearly flat structure. This unique layout yields excellent stability for the molecule and makes it easy for bacteria to link to its active sites [37].

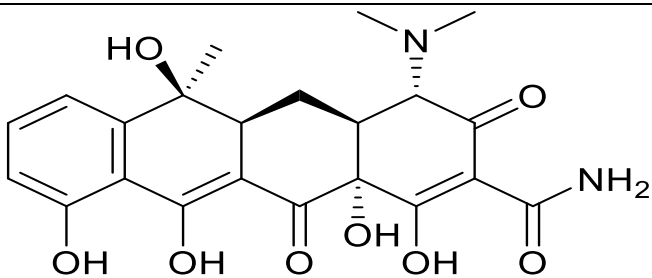
TC has several functional groups that play essential roles in both chemical and biological properties. One of the most prominent, carbonyl groups, which augment the molecule's polarity and give it unique chemical properties. In addition, it is soluble in water because of the presence of hydroxyl groups. Moreover, there is an amine and amide group that endows this compound with some basic properties [38].

The particular design of this structure and the presence of these functional groups indicate that TC can effectively interact with proteins and bacterial DNA directly, thus preventing protein synthesis, causing bacteria to stop reproduction, and ultimately killing them [39].

TCs have their own unique set of physical and chemical properties. It is a crystalline powder at room temperature; in solid form, it is yellow or green–yellow and soluble in water. It also has acidic properties, so it can react with other compounds in the surrounding environment. Spectroscopic absorption methods quickly detect it because it absorbs in the UV region. Despite its stability, tetracycline is highly sensitive to both light and heat. Table 1.1 shows the chemical structure and general properties of the tetracycline molecule [40].

Table 1.1

Tetracycline specifications

Name	Tetracycline
Chemical structure	
IUPAC name	(4S,4aS,5aS,6S,12aR)-4-(dimethylamino)-1,6,10,11,12a-pentahydroxy-6-methyl-3,12-dioxo-4,4a,5,5a-tetrahydrotetracene-2-carboxamide
Molecular weight	444.4 g/mol
Chemical formula	C ₂₂ H ₂₄ N ₂ O ₈
Solubility in water	Freely soluble in water 231 mg/L (at 25 °C), methanol, ethanol. Insoluble in ether, hydrocarbons.
Color/Form	Yellow/Crystalline Powder
pH	3.0-7.0
λ _{max}	356-358 nm (for water solutions)

TC, which is widely used as an antibiotic in human and veterinary medicine, is now considered a persistent and dangerous environmental pollutant, especially since tetracycline is the second most widely used antibiotic in the world according to 2020 [41], as it is estimated that daily human consumption of tetracycline worldwide is approximately 23 kg [42], and as a result of its continuous consumption, excessive use and poor ability to decompose, it has become a major threat to the environment [42], as it is now present in surface and groundwater, as well as in wastewater, owing to its discharge through urine and feces after its use by humans and animals and the ineffectiveness of traditional water treatment techniques in removing it, it often leaks into many aquatic environments, leading to significant negative effects on living organisms.

Given the significant challenges associated with the presence of TC and its residues in water, this work investigated the effective removal of tetracycline from water, which requires the adoption of advanced and innovative methods and the development of new and more effective treatment technologies, especially since TC is characterized by its chemical stability and slow decomposition, which makes it difficult to remove via traditional methods.

1.3 Water treatment techniques

TC is challenging to remove from water because it has very stable chemical properties and does not easily breakdown. This arises from the tendency of tetracycline to form stable complexes with metal ions such as calcium. Furthermore, tetracycline breaks down exceptionally slowly at specific pH values. This leads to the accumulation of tetracycline in water sources, posing health risks to living organisms and leading them toward doom [43]. Therefore, it is essential to develop new technologies for treating tetracycline-contaminated water and thus reducing its environmental impact.

Over the years, TC treatment technologies have become more varied, replacing traditional methods. These technologies range from physical, chemical, and biological processes [44]. Filtration is one of the initial water treatment methods, in which tetracycline and other pollutants are filtered out via micro- or nano membranes [45]. Although it effectively removes small particles, filtering liquids requires regular maintenance and is costly, and over time, membranes become clogged with matter, reducing their effectiveness and increasing replacement costs [46].

Next, reverse osmosis, a technology that relies on passing water under high pressure through a semipermeable membrane to separate contaminants, was used [47].

Reverse osmosis is effective in removing a wide range of contaminants, including TC, but it requires much energy to pump water under the necessary pressure, making it expensive to operate. In addition, this technology produces large quantities of water, which is largely wasted. Additionally, it is not limited to removing contaminants only; it also removes most of the minerals in water, and its maintenance costs are high and complex [48], which makes it an unwanted technology.

The focus then shifted to adsorption, a technique that relies on the use of absorbent materials such as activated carbon and natural clay to absorb pollutants from water [49]. Adsorption is considered one of the most effective methods for removing TC due to the high ability of these materials to capture organic pollutants from water [50]. It is also an easy-to-apply technique and relatively less expensive than some other techniques, but it requires replacing the absorbent materials regularly when they become saturated [51].

Recently, new advanced techniques using nanomaterials have been developed, which has revolutionized science. One of these methods is photodegradation, which uses photocatalysts such as zinc oxide (ZnO) or titanium dioxide (TiO₂) to break down TC molecules into harmless substances with the help of light [52]. This approach is highly effective because it completely removes pollutants without producing harmful byproducts [53].

The best way to ensure the effective removal of TC from water is by using a combination of different technologies [54]. The selection of the right treatment method depends on many factors, such as the concentration of TC, the cost of the treatment, the effectiveness of the method, and the environmental impact. Advanced oxidation technologies, including photodegradation, are highly efficient for the complete removal of TC [55], whereas adsorption methods are suitable for cases that require economical, simple, and easy-to-apply solutions [50]. In general, sometimes, a single technology may not be sufficient to achieve effective treatment, requiring the combination of two technologies to achieve high efficiency and effectiveness in removing pollutants from water.

1.3.1 Adsorption technique

Adsorption is the process of the accumulation of molecules or atoms, whether liquid, gaseous or dissolved solids, on the surface of a solid, resulting in the formation of a thin layer of these adsorbed molecules on the surface of the adsorbent [56].

This surface phenomenon occurs when physically or chemically attractive forces interact with molecules or atoms in the surrounding medium, causing them to adhere to the surface of the solid [57]. This process differs from absorption, as absorption occurs when molecules or atoms completely penetrate the adsorbent and become part of its internal structure [58].

Depending on the nature of the force between the adsorbed molecules and the adsorbent molecule, adsorption can be divided into physical and chemical adsorption [59]. Physical adsorption occurs when molecules are attracted to the surface of a solid through weak forces, including van der Waals forces. Such forces cannot make lasting bonds between molecules so that this process can be reversed. The bonds that have emerged to attract these molecules onto surfaces are broken without the need for high energy [61]. In contrast, chemical adsorption involves the formation of stronger chemical bonds between molecules and a surface, making it both more stable in nature and difficult to reverse [60]. The adsorbed molecules are given up with more difficulty; as a result, this adsorption results in the formation of thin layers on the surface [61].

Adsorption is an efficient and widely used method. In addition, it is simple, flexible technique and can be used under various circumstances without complicated techniques; this makes it suitable for a wide variety of environments [62]. Compared with other methods, this method is also inexpensive because the materials used in adsorption are generally easy to find and cheaply purchased. Additionally, these materials have large surface areas [63]. Thus, the pollutant molecules can interact with many active sites on the surface, leading to the adsorption of a large number of pollutants effectively. All these advantages make it a desirable and practical method, especially for use in industrial and environmental aspects such as water purification [64].

Adsorption is highly effective in eliminating many kinds of pollutants from drinking water and wastewater. Organic pollutants such as TC and inorganic pollutants such as heavy metals such as mercury, lead, and cadmium can be effectively removed by

adsorption [65]. The success of the process is determined by a number of factors, including the type and properties of the adsorbents used, the properties of the pollutant substances, the temperature, and the pH of the environment [65]. However, adsorption remains one of the best ways to clean up water if the right adsorbents and optimal conditions for adsorbing pollutants are used.

1.3.1.1 Adsorbent materials

Adsorbents are efficient materials for removing most types of pollutants from water. There are different types on the basis of their features and nature. Some are natural, such as clay, zeolite, and natural coal. They are popular, mainly because they are easy to find in nature and inexpensive [66]. Another type is industrial, such as activated carbon and silica gel. They are often made from waste or byproducts of industry or agriculture, and they are modified to improve the efficiency of pollutant adsorption [66].

The elimination of pharmaceutical pollutants such as TC from water is a major environmental challenge. Therefore, various adsorbents have been used and have shown high efficiency. Clays such as bentonite [67], montmorillonite [68], and kaolinite [68] are effective because of their high porosity and strong adsorption capacity. Other materials, such as activated carbon [69], carbon nanotubes [70], and graphene oxide [71], have also proven to be highly efficient in removing TC from water and improving water purification.

1.3.1.1.1 Clay

Clay is a naturally occurring earthy material found in the Earth's crust and is composed of very fine-grained minerals [72], usually less than 2 micrometres in size [73]. Clay is formed as a result of the erosion of rocks containing the feldspar mineral group [72], which is a group of minerals that are the main component of rocks and constitute approximately 60% of the composition of the Earth's crust [74].

When feldspar minerals are exposed to chemical weathering, they decompose and turn into clay minerals, which occurs mainly because of their interaction with water and natural acids in the soil and environment, where the weathering process over long periods of time leads to the formation of clay minerals such as kaolinite (the main minerals in kaolin clay) and montmorillonite (the main minerals in bentonite clay) and other minerals such as chlorite and vermiculite [75].

Clay minerals mainly include hydrated aluminum silicate $\text{Al}_2\text{Si}_2\text{O}_5(\text{OH})_4$ (containing silicon, aluminum, oxygen, and water) in addition to other minerals, such as iron, magnesium, alkali metals, and other cations [72].

Clay minerals have a sheet-like structure and consist mainly of tetrahedral silicate groups (silicon atoms surrounded by four oxygen atoms forming a pyramid-like structure) and octahedral aluminate groups (aluminum or magnesium atoms surrounded by oxygen or hydroxyl (OH) atoms), where these sheets are connected to each other to form different types of clay minerals [76]. The tetrahedral and octahedral sheets are illustrated in appendix A1 [77].

Clay minerals can be classified as 1:1 or 2:1. When a tetrahedral plate is bonded to an octahedral plate, a 1:1 clay mineral is produced; kaolinite is an example of this. A 2:1 clay consists of an octahedral plate sandwiched between two tetrahedral plates, and bentonite is an example of this [78]. The 1:1 and 2:1 ratios of clay minerals are listed in appendix A2 [79].

Clay can also be divided into two types. Expandable clay is characterized by its ability to absorb water or other liquids, which leads to an increase in its volume, as it is characterized by changes in the distance between the mineral layers when exposed to water or other materials. This type of clay, such as smectite, is widely used in water purification [75].

The other type is nonexpandable clay, which is clay that does not absorb large amounts of water or liquids; therefore, its volume does not change because it lacks the flexible layered structure that allows liquids to enter between the layers. It is widely used in the ceramic and construction industries, such as illite [75]. The two types of 2:1 clay minerals are described in appendix A3 [80].

The electrical charge in clay plays a key role in determining how the clay reacts to various contaminants. There are two main types of charges in clay minerals. Structural charge, which is a permanent charge that arises within clay layers as a result of replacing some ions in the clay structure. For example, another ion (such as magnesium or iron) can replace the original ions (such as silicon or aluminum) in the crystal lattice without affecting the clay structure. This results in the formation of a permanent negative charge, and this charge contributes to the ability of the clay to attract positive ions from the

surroundings. The other type is surface charge, which is a variable charge that depends on the pH of the environment and results from the hydrolysis of Si–OH or Al–OH bonds. When the pH is less than zero (pH_{pzc}), clay typically has a positive surface charge, which leads to attraction to molecules that have opposite charges (anions). However, if the pH increases beyond pH_{pzc} , the surface charge on the clay becomes more negative, so it can attract and react with positively charged ions [76].

In 1:1 clay, most of the total charge comes from the surface charge. In 2:1 clay, most of the charge is structural charge, whereas the surface charge contributes to less than 1% of the total charge. This disparity in charge distribution affects how clay reacts with ions and pollutants and its effectiveness in various applications, such as water treatment [76].

Clay is commonly used in water purification. Its structure allows it to efficiently adsorb undesirable substances, such as heavy metals, dyes, and organic compounds. Clay has this extraordinary capacity, mainly because of its unique crystalline structure, high surface area, and exchangeable ions on its surface [81].

There are several ways in which contaminants interact with clay molecules, the most important of which are physical adsorption, chemical interaction, ion exchange, and hydrogen bonding, as each of these methods depends on the nature of the contaminants and the type of clay used, which makes clay a multifunctional and effective material for treating many contaminants in different environments with high efficiency and effectiveness [81].

1.3.1.1.1 Bentonite

Bentonite is a soft clay composed mainly of montmorillonite, which is a hydrated aluminum silicate that contains magnesium, sodium and calcium; it may also contain iron $(\text{Ca,Na})_{0,3}(\text{Al,Mg})_2 \text{Si}_4\text{O}_{10}(\text{OH})_{2-n} \text{H}_2\text{O}$. Bentonite belongs to the smectite group of clay minerals (2:1-layer minerals). This clay is formed when volcanic ash is exposed to water for a long period of time, converting the volcanic glass particles into clay minerals that are most similar to bentonite [82]. The basic structure of bentonite is shown in appendix A4 [83].

Bentonite is an absorbent swell clay, meaning that it has a high ability to absorb water. Therefore, when it absorbs water, its volume significantly increases, and it swells

simultaneously. This property is created because of its layered mineral composition, where water molecules are located between its layers. Bentonite can be divided into two main types on the basis of its dominant cations: sodium bentonite and calcium bentonite [84].

Because it can swell and absorb, sodium bentonite is particularly good at absorbing substantial amounts of water. It is the first choice for a variety of applications, such as well drilling, seepage control in dams, and sewage treatment, in addition to many different areas, such as the cement concrete industry [85]. In contrast to sodium bentonite, calcium bentonite does not swell and absorbs less water but has exceptionally efficient impurity removal capacities. For this reason, it is a good choice for detoxifying and purifying water [86].

The unique adsorption and structural properties, ion exchange, excellent chemical stability, large surface area, and nontoxicity of bentonite contribute to its efficiency. Moreover, bentonite is abundant, economical, and safe, and it can also be reused numerous times with minimal reduction in effectiveness; therefore, it provides an excellent choice for an environmentally sustainable water treatment solution [87].

In recent decades, public attention to improving water treatment methods has increased. The most prominent of these is the use of bentonite composites with photocatalysts for environmental protection [88]. Earlier studies have shown that the combination of adsorption and photodegradation is an effective method for removing pollutants from water. A large surface area is the key to the high adsorption capacity of bentonite, providing more active sites where contaminants can interact with catalysts. Moreover, photodegradation breaks down these pollutants via the use of photocatalysts such as TiO_2 and ZnO . This combination greatly improves the efficiency of purifying water [88, 89].

1.3.2 Photodegradation

Photodegradation means that large molecules become small, nontoxic molecules. The process consists of using sunlight as energy and oxidation–reduction reactions to obtain molecules of lower molecular weight. In addition, it is also a promising technology because it converts light energy to chemical energy. This makes it practical for many uses at high efficiency [90].

It is widely used in many environmental applications, such as water purification, because of its effectiveness in treating many pollutants, such as antibiotics and other chemicals. It is an effective alternative to traditional methods, as it is an environmentally friendly technology [90].

On the other hand, reactions that include catalysts to accelerate them are known as photocatalysis, which increases the effectiveness of the process and removes pollutants faster and more efficiently [90].

1.3.2.1 Photocatalysis

In the early 1970s, the phenomenon of photocatalysis received special attention when Fujishima and Honda reported that water could be decomposed with light via a photocatalyst; this discovery recently expanded the applications of photocatalysis and its use in public areas such as water purification [91].

A catalyst is a substance that accelerates the reaction by providing a new path with lower activation energy without being consumed in the reaction process, and it is called a photocatalyst because it relies on light as an energy source to stimulate the chemical reaction [93].

Photo-catalysis can be classified into two main types, homogeneous and heterogeneous, according to the phase (physical state) of the catalyst used rather than the reactants. In homogeneous photocatalysis, the catalyst is in the same phase as the reactants, often a liquid phase in this case, where the catalyst is dissolved in a solution containing contaminants, such as the Fenton photosystem. In contrast, in heterogeneous photocatalysis, the catalyst is in a different phase than the reactants. In most cases, the catalyst is in a solid state, whereas the reactant is in a liquid or gaseous state. Semiconductors and some transition metal oxides are the most common heterogeneous catalysts, acting as solid catalysts for the decomposition of contaminants in the liquid or gaseous phase [92].

Semiconductors have electrical conductivity that lies between that of conductors (such as metals) and insulators (such as glass). Some semiconductors (such as TiO₂, ZnO, ZnS, CdS and Fe₂O₃) have a filled valence band and an empty conduction band. Electrons are usually found in the valence band, which is the highest energy band representing filled energy levels, whereas the conduction band is the lowest energy band, which is empty of

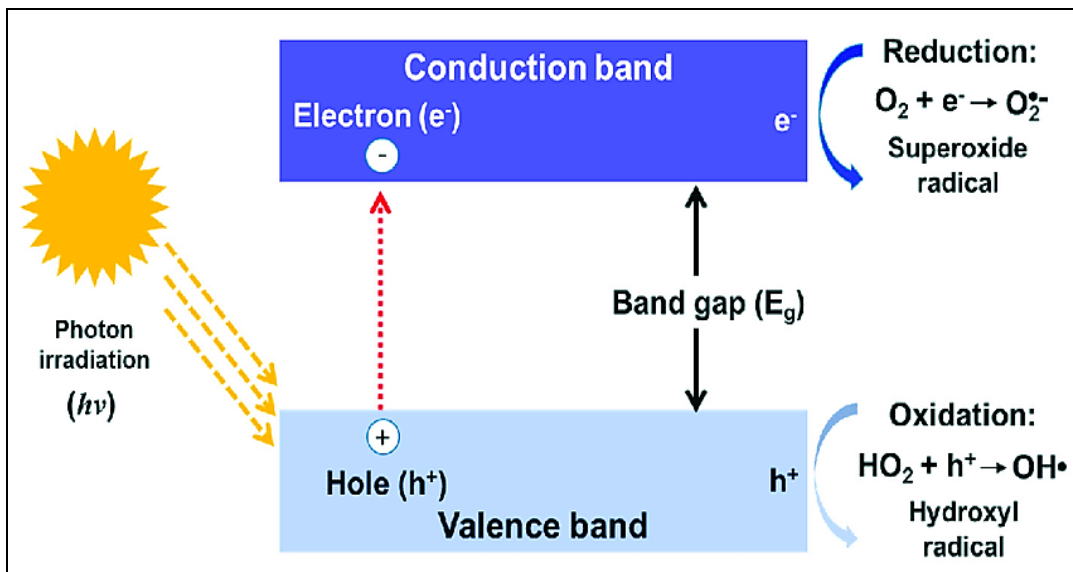
electrons. The band gap separates these two bands, which is the energy required to stimulate an electron to move from the valence band to the conduction band [94].

In photocatalysis, when semiconductors are exposed to light with sufficient energy (greater than or equal to the energy bandgap), photons are absorbed, causing electrons to move from the valence band to the conduction band, creating a free electron in the conduction band and leaving a positive hole in the valence band [94].

These electrons and holes participate in oxidation and reduction reactions with contaminants present on the surface of the catalyst, where an oxidation reaction occurs between holes and reducible molecules, and a reduction reaction occurs between excited electrons and oxidizable molecules through a series of reactions that lead to the decomposition of these contaminants into harmless substances such as water and carbon dioxide [94]. The photocatalysis reaction is shown in Figure 1.1 [95].

Figure 1.1

Semiconductor after irradiation with light in the photocatalysis reaction



In the oxidation reaction, the positive holes react with H₂O molecules near the surface and generate a hydroxyl radical ([•]OH), as shown in equation (1.1) [94]. On the other hand, in the reduction reaction, the electrons react with O₂ molecules to produce superoxide ions ([•]O₂⁻), as shown in equation (1.2) [94]. Hydroxyl radicals and superoxide are highly reactive molecules with a high oxidizing capacity, leading to the breakdown of harmful organic compounds and pollutants, as shown in equation (1.3) [94].



Semiconductors play a major role in many modern applications, from converting light into electricity to photocatalysis for water purification and pollutant treatment, as they are promising solutions that combine efficiency and reliance on clean energy sources, making them effective tools for combating pollution and improving water and environmental quality.

1.3.2.1.1 ZnO semiconductor photocatalyst

Zinc oxide (ZnO) is an inorganic chemical compound that is a white powder in its natural state, is insoluble in water but soluble in acids and bases, and is one of the most common oxides used in many industrial applications, such as cosmetics, nutritional supplements, ceramics, plastics, cement, glass, and semiconductors [96]. ZnO is usually found in two main crystal structures: hexagonal (wurtzite) and cubic (zincblende), but the hexagonal structure is the most common and stable under natural conditions [96].

ZnO is an n-type semiconductor and has a wide band gap of approximately 3.3 electron volts (eV) at room temperature, which allows it to absorb in the ultraviolet region, and it also shows activity under sunlight [97], since approximately 5% of the solar spectrum falls in the ultraviolet region [98], making it useful in applications that require interactions with light, such as photocatalysis [96].

ZnO is one of the most prominent materials used in photocatalysis, as it has a set of properties that make it a unique photocatalyst compared with other semiconductors. Among these properties is the wide band gap that allows it to absorb high-energy photons from ultraviolet rays, and it has a high ability to generate the electrons and holes necessary to cause chemical reactions on the surface, in addition to its low cost owing to its abundance, nontoxicity, strong oxidizing nature, chemical stability, and inability to corrode easily, which makes it ideal for use in different environmental conditions [99]. These advantages make it one of the best options for treating water from pollutants.

1.4 Aims of the study

The main objective of this study was to develop an efficient and low-cost technology for purifying water from organic antibiotic residues such as tetracycline by combining adsorption and photodegradation methods via simulated sunlight. ZnO nanoparticles can be used as safe and low-cost semiconductors. Moreover, ZnO combines with bentonite, a safe support material, to form a composite catalyst. Efficiency, effectiveness, and determine the ideal conditions will be assessed for the process.

This is the first study reporting the use of a ZnO/bentonite composite catalyst for water purification from tetracycline by adsorption and photodegradation techniques under simulated sunlight.

This study was designed to synthesize a novel ZnO/bentonite composite, and this is the main objective. Another goal of this work is to characterize ZnO/bentonite by X-ray diffraction (XRD), scanning electron microscopy (SEM), energy dispersive X-ray spectroscopy (EDX), and other advanced techniques. We evaluated the degradation efficiency of tetracycline by the ZnO/bentonite composite in water under simulated sunlight. We investigated the influences of different environmental factors, such as pH, the pollutant concentration in water, the catalyst amount, the temperature, and the presence of oxygen and carbon dioxide, to understand what role these conditions play in the activity of this catalyst. Furthermore, we will ascertain whether the composite can be reused without significant loss of efficiency.

Chapter Two

Experimental

2.1 Materials and Instruments

2.1.1 Chemicals

All chemicals, including commercial zinc oxide (ZnO) powder, zinc acetate dihydrate ($\text{Zn}(\text{OOCCH}_3)_2 \cdot 2\text{H}_2\text{O}$), bentonite clay ($\text{Al}_2\text{H}_2\text{O}_6\text{Si}$), tetracycline hydrochloride powder ($\text{C}_{22}\text{H}_{24}\text{N}_2\text{O}_8 \cdot \text{HCl}$), sodium hydroxide (NaOH), hydrochloric acid (HCl), sodium chloride (NaCl), and calcium carbonate (CaCO_3), were purchased from Sigma–Aldrich. These materials were used in their original state without any modification or further preparation.

2.1.2 Equipment

An Ohaus AV264 C analytical balance was used to measure the exact masses of the chemicals in all the experiments. Different solutions required for the experiments were prepared via different volumetric flasks (100, 250 and 1000 ml). Photolysis experiments were performed by placing the samples in 250 ml beakers. A low-speed centrifuge LLS-A12 was used to prepare the samples for analysis. A Corning 6795-420D PC-420D Stirring hot plate with digital displays was used to stir and heat the solutions during the preparation of the different compounds. A bench top muffle furnace was used to anneal the prepared compounds. Laboratory porcelain mortar with pestle was used to grind the compounds into very fine powders after preparation. The effect of pH was studied by measuring it via a Jenway™ 35459-02 device. A Labtech shaker (Daihan Labtech) LSB-015S was used to ensure that the solutions were well mixed to obtain more accurate pH readings. The effect of oxygen was studied by pumping it with a SHANDA SD 900 oxygen pump. A mercury-filled chemical thermometer (30 cm long) was used for the temperature measurements. A MEDIUM-536P solar simulator with two so2853 lamps with a power of 400 W was used as the light source for the photolysis experiments. An Extech Model 401025 Digital Candle/lux 3 Range Light Meter was used to measure the light intensity. Faithful SH-4 5000 ml hotplate magnetic stirrer ceramic top plate heavy duty tops were used for continuous stirring of the solutions during the photolysis experiments. The tetracycline concentration was measured with a spectrophotometer (UV-1800 UV–VIS. Shimadzu).

For the complete tetracycline mineralization experiment, a Waters 1525 H.P.L.C. was used, and an FT-IR Nicolet IS5 (Thermo Fisher) was employed to monitor the degradation of tetracycline. The crystal structure, morphology and structural properties of ZnO, bentonite and the composite catalyst were studied via X-ray diffraction (XRD), scanning electron microscopy (SEM), and energy-dispersive X-ray spectroscopy (EDX). All these analytical techniques were used in South Korean laboratories.

2.1 Preparation of Solutions

2.1.1 Stock solution

To prepare a stock solution of tetracycline at a concentration of 1000 ppm, 0.0999 g of tetracycline was weighed accurately and then dissolved in distilled water. After ensuring complete dissolution, the solution was transferred to a 100 ml volumetric flask, and the volume was completed with distilled water to the mark.

Tetracycline solutions at different concentrations of 10, 20, 30, 40, and 50 ppm were prepared from the stock solution, where 1, 2, 3, 4, and 5 ml, respectively, were removed via a volumetric pipette, each quantity was transferred to a 100 ml volumetric flask, and the volume in each flask was filled with distilled water to obtain the desired concentration.

2.1.2 Other solutions required

The following solutions were prepared and used for the experiments:

1. A 0.9 M NaOH solution was prepared by dissolving 8.99 g of NaOH in 250 ml of distilled water.
2. A 0.40 M zinc acetate solution was prepared by dissolving 8.78 g of zinc acetate in 100 ml of distilled water.
3. A 0.01 M NaCl solution was prepared by dissolving 0.372 g of NaCl in 500 ml of distilled water.

2.2 Preparation of the ZnO/bentonite composite catalyst

To support zinc oxide on bentonite, 10.00 g of bentonite clay was added to 250 ml of 0.9 M sodium hydroxide solution, and the mixture was heated at 55 °C with continuous stirring. Then, 100 ml of 0.40 M zinc acetate solution was added dropwise for 2 h. The resulting solid was decanted and washed continuously with distilled water until the

liquid became neutral. Then, the solid was dried and annealed in an oven at 250 °C for 1 h. After that, it was finely ground in a mortar to very fine granules and stored for use.

2.3 Photo-catalytic system and parameter effects

2.3.1 Photo-catalytic system

The light source was assembled above the sample and was set at a fixed distance above the reactor of approximately 70 cm, and the light intensity was controlled using a lux meter, where the average measured solar light intensity was approximately 10000 lux, which is equivalent to the intensity of natural sunlight. The lamp has a stable and high brightness of 5200 lumens, covers a wide spectral range (200-800 nm), and has a radiation density of approximately 0.0146 W/cm².

The photolysis reaction was carried out in a 250 ml beaker containing the composite catalyst and a water sample previously contaminated with the antibiotic (tetracycline), and the reactor was continuously magnetically stirred to ensure an even and good distribution of the catalyst across the sample. The change in the tetracycline concentration was measured over time, where small samples of the solution were taken from the reaction vessel every 15 min for 90 min (30 min in the dark, 60 min under light) and then centrifuged (4000 rpm for 3 min). The reaction was conducted at room temperature (25 °C) and at a pH of 8.5.

2.3.2 Effect of catalyst amount

The effect of catalyst quantity on the photodegradation process was studied. Different amounts of ZnO/bentonite catalyst (0.050, 0.100, 0.200, 0.300, 0.400 and 0.500 g) were mixed with 100 ml of tetracycline at a concentration of 40 ppm for 90 min (the adsorption of tetracycline on the catalyst occurred during the first 30 min in the dark, after which the photodegradation step started) at the temperature and pH mentioned above.

2.3.3 Effect of initial tetracycline concentration

The effect of changing the concentration of tetracycline on the photodegradation process was studied. Different concentrations of tetracycline (10, 20, 30, 40 and 50 ppm) in 100 ml were prepared and mixed with 0.100 g of the ZnO/bentonite catalyst for 90 min.

2.3.4 Effect of pH

The photodegradation process was studied when the pH of the medium was changed. The experiments were carried out using 100 ml of tetracycline at a concentration of 40 ppm with 0.100 g of the ZnO/bentonite catalyst for 90 min, and the pH was controlled before starting the experiment by adding a few drops of sodium hydroxide or hydrochloric acid to obtain different pH values (in acidic media 3.0 and 5.3 and basic media 8.5 and 10.1 and neutral media 7.0).

2.3.5 Effect of temperature

The photodegradation process was studied when the initial temperature of the reaction medium was changed. The experiments were carried out using 100 ml of tetracycline at a concentration of 40 ppm with 0.100 g of the ZnO/bentonite catalyst for 90 min, and the temperature was controlled before starting the experiment by adding hot water or ice around the reactor beaker to obtain different temperatures of 7, 15, 25, 30 and 57 °C.

2.3.6 Effect of oxygen

The effect of adding oxygen to the reaction medium on the photodegradation process was studied. The experiment was conducted using 100 ml of tetracycline at a concentration of 40 ppm with 0.100 g of the ZnO/bentonite catalyst for 90 min, where oxygen was pumped into the reaction medium throughout the experiment after ensuring that the pumping tube was well fixed in the beaker.

2.3.7 Effect of carbon dioxide

The effect of adding CO₂ to the reaction medium on the photodegradation process was studied. A total of 100 ml of 40 ppm tetracycline was added to 0.100 g of ZnO/bentonite catalyst for 90 min. CO₂ gas was produced by reacting 4.10 g of calcium carbonate (CaCO₃) with 50 ml of water and then adding 5 ml of concentrated hydrochloric acid (HCl). The CO₂ formed was then pumped into the reaction medium via the glass tube system, which was tightly closed; this ensured that the solution remained gas saturated throughout the experiment.

2.3.8 Recovery of the catalyst and reuse

To evaluate the efficiency of the ZnO/bentonite catalyst, 0.100 g of the catalyst was mixed with 100 ml of (40 ppm) tetracycline solution for 90 min. After the reaction was

completed, the catalyst was separated by washing three times with distilled water to remove any impurities or residues from the previous reaction, after which it was easily separated from the solution via decantation. Then the catalyst was filtered to ensure complete cleanliness and then dried at room temperature to ensure readiness for reuse.

The catalyst was reused with fresh tetracycline solution of the same concentration, volume and conditions. These steps of separation, washing, filtration, drying, and reuse were repeated for five consecutive cycles.

2.3.9 Complete mineralization

To confirm the complete mineralization of tetracycline by the catalyst, 0.100 g of ZnO/bentonite catalyst was mixed with 100 mL of 40 ppm tetracycline solution for 180 min. Samples were taken from the solution every 30 min to analyze the reaction progress and then examined via different analytical techniques, namely, FT-IR, UV-Vis and high-performance liquid chromatography (HPLC), to determine the degradation efficiency.

2.4 Control experiments

2.4.1 In the absence of a catalyst

Without the catalyst, 40 ppm tetracycline solution (100 ml) was placed in the dark with stirring for 30 min and then under simulated sunlight for 60 min. The concentration was measured before and after exposure to light.

2.4.2 In the dark

Three experiments were conducted to evaluate the effectiveness of tetracycline removal in the absence of light. The first experiment involved 0.1 g of ZnO, the second experiment involved 0.1 g of bentonite, and the third experiment involved 0.1 g of ZnO/bentonite as a catalyst. In all the experiments, 40 ppm tetracycline solution (100 ml) was used with continuous stirring for 90 min, and the concentration was measured before and after the experiments.

2.4.3 In light

Three experiments were conducted under light. The first experiment involved the use of 0.1 g of ZnO as a catalyst, whereas the second experiment involved the use of 0.1 g of bentonite as an adsorbent. In the third experiment, 0.1 g of the catalyst ZnO/bentonite was used. For all the experiments, a tetracycline solution was prepared at a concentration of 40 ppm (100 ml) and was continuously stirred under light for 60 min (after being placed in the dark for 30 min). The concentration was measured before and after exposure to light to determine the effectiveness of both the individual compounds and the composite system in removing tetracycline.

2.5 Zero-point charge

The pH_{pzc} values and surface charges of various solids were determined via the pH drift method. A 0.01 M solution of NaCl was boiled to remove dissolved carbon dioxide gas, which may affect the pH value. The solution was then cooled to 25 °C. NaCl solutions (20 ml) were distributed into three sets of six 50 ml glass bottles. The pH of the solutions in these bottles was adjusted to specific values ranging from 2-12 by adding small amounts of dilute NaOH or HCl solutions as needed. The initial pH values were determined first. In the first set of bottles, 0.1 g of ZnO was added, 0.1 g of bentonite clay was added to the second set of bottles, and in the third set, 0.1 g of ZnO/bentonite catalyst was added. The bottles of each set were put into a thermostatic shaker and shaken at 25 °C for 24 h. Finally, the final pH values were measured.

Chapter Three

Results and discussion

This chapter displays the impacts of various factors, such as temperature, pH, oxygen, carbon dioxide, pollutant concentration and catalyst amount, on photodegradation and adsorption processes in removing tetracycline from water via ZnO/bentonite. The results of the characterization of the catalyst and its components were also analyzed, which provides valuable insights into the nature and properties of the catalyst. In addition, the results of the catalyst reuse and complete mineralization of tetracycline were discussed, and this analysis led to an understanding of the potential of this composite in water treatment. All the data were processed via OriginPro 8.5 software, and these results were compared with those of previous studies.

3.1 Characterization results

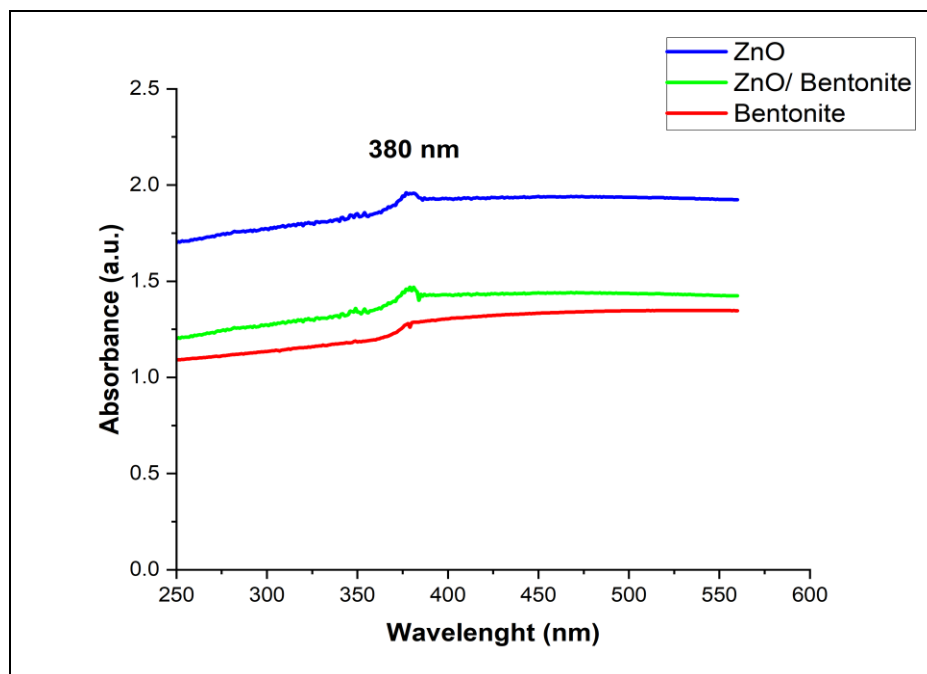
3.1.1 UV–Vis

As an indispensable method in recent research, ultraviolet–visible (UV–Vis) absorption spectroscopy is a powerful technique for examining the optical and photoelectronic properties of solid materials. It allows researchers to judge a material's ability to absorb light across a wide range of wavelengths, offering important data on its properties. This information is essential for assessing the catalyst efficiency in photodegradation.

Figure 3.1 presents the absorption UV–Vis spectra of ZnO, bentonite, and the catalyst composite. The spectrum of both the ZnO and the composite reveals a strong absorption peak at approximately 380 nm, indicating that they can absorb UV photons. Consequently, these materials are useful for photocatalytic applications under sunlight, as 5% of the total solar energy comes from UV radiation. In the composite spectrum, no significant shift in the absorption peak was observed, suggesting that bentonite has little effect on the optical properties of ZnO. Moreover, bentonite does not show any peak, indicating that the observed phenomena mainly arise from the ZnO particles.

Figure 3.1

Solid-state electronic absorption spectra measured for ZnO powder, bentonite and ZnO/bentonite. Measurements were performed using a tetracycline solution (40 ppm, 100 ml) with 0.1 g of the catalyst. Baseline correction was made with distilled water



The observed absorption wavelengths of ZnO and the ZnO in the composite system closely align with the values reported in previous studies [100], which strengthens the reliability of the electronic properties of the prepared composite.

3.1.2 X-ray diffraction (XRD) patterns

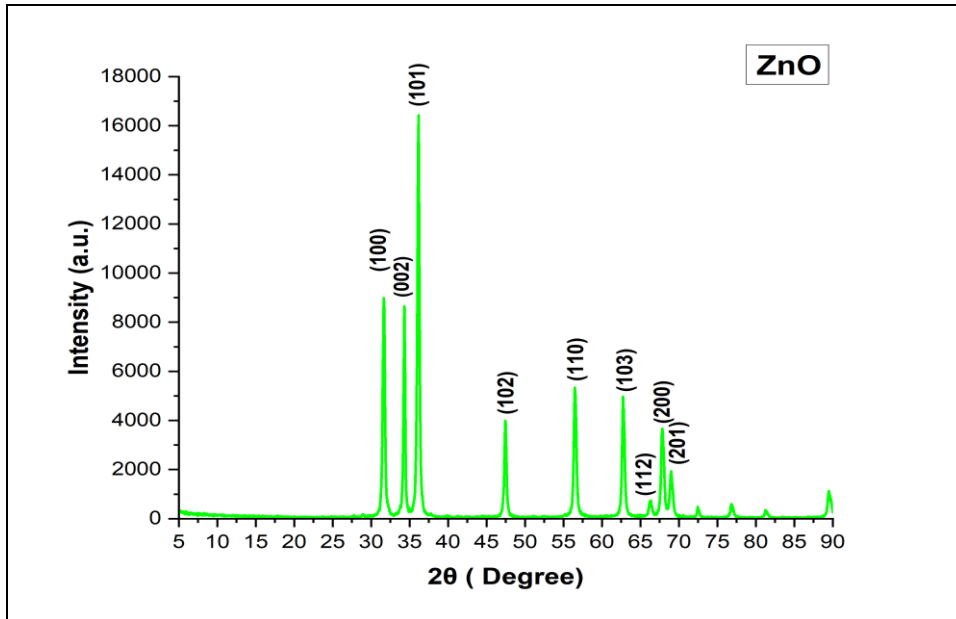
XRD is an essential technique for examining the crystalline structure of materials. It helps identify the type of crystalline material, determine the size of the crystalline particles, detect impurities, and reveal the atomic arrangement. The XRD pattern of the ZnO sample was measured as shown in Figure 3.2.

The results revealed the presence of major diffraction peaks at the following diffraction angles (2θ): 31.2° , 33.9° , 36.6° , 47.0° , 56.2° , 62.5° , 66.5° , 67.6° and 68.7°

These peaks are due to reflections from the (100), (002), (101), (102), (110), (103), (112), (200) and (201) crystal planes, respectively.

Figure 3.2

X-ray diffraction pattern of the ZnO powder



These peaks are consistent with the reference card (JCPDS-79-2205). This indicates the presence of a hexagonal wurtzite structure of ZnO, which is consistent with previous studies [100]. This confirms the purity of the sample and its unique crystalline properties.

The average crystal size was calculated via the Scherrer equation [101], as shown in equation 3.1:

$$D = \frac{K \lambda}{\beta \cos(\theta)} \quad (3.1)$$

where D is the average crystal size (nm), K is the shape factor (0.94), λ is the X-ray wavelength (0.15418 nm), β is the width of the peak at mid-height in radians, and θ is the Bragg angle (half-angle 2θ).

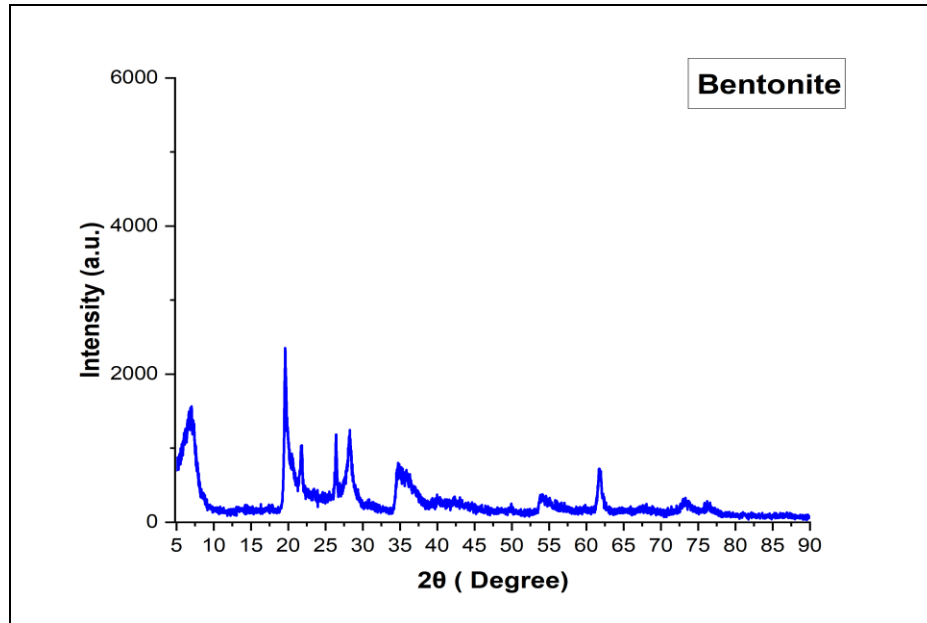
On the basis of calculations of the main (100), (002) and (101) peaks, the average crystal size was estimated to be approximately 26 nm.

These results confirm that ZnO powder has a nanostructure with a hexagonal crystal arrangement (wurtzite structure), which makes it suitable for use in photocatalysis because of its unique properties.

The XRD pattern of bentonite clay was measured as shown in Figure 3.3, where the pattern shows peaks at angles of 6.28°, 19.9°, 21.9°, 26.7°, 27.7°, 35.4°, 54.4° and 61.8°.

Figure 3.3

X-ray diffraction pattern of bentonite clay



The interatomic distance of bentonite was calculated via Bragg's law [102], as shown in equation 3.2:

$$D = \frac{n \lambda}{2 \sin(\theta)} \quad (3.2)$$

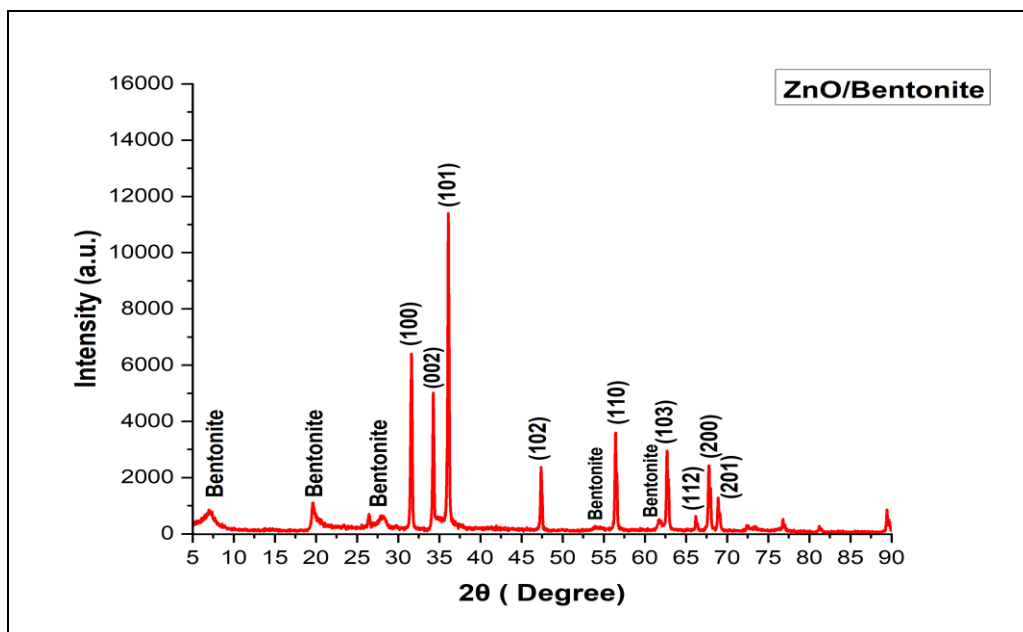
where D is the distance between adjacent atomic layers in the crystal (nm), θ is the Bragg angle, λ is the wavelength of the incident X-ray (0.15418 nm), and n is an integer (diffraction order, n =1).

On the basis of this law, the distance between the atomic layers in bentonite clay was 1.5 nm. Calculating this distance is essential for analyzing the crystal structure of bentonite at the nanoscale, as it provides important information about the atomic arrangement in the material. This information contributes to understanding the physical and chemical properties of bentonite, such as its ability to absorb and interact with other materials.

The XRD pattern of the ZnO/bentonite composite was measured, as shown in Figure 3.4. The patterns showed all the characteristic ZnO peaks, such as (100), (002), and (101), clearly indicating the presence of ZnO particles on the surface of the bentonite.

Figure 3.4

X-ray diffraction pattern of the ZnO/bentonite composite



The interlayer distance of the ZnO/bentonite crystal was calculated to be 1.5 nm via Bragg's law. This value agrees with the value for pure bentonite, indicating that the ZnO particles remained exclusively on the surface of the bentonite and did not penetrate it in any way.

The bentonite peaks in the composite material, observed at 2θ values of 6.28° , 19.9° , 26.7° , 27.7° , 54.4° , and 61.8° , indicate that there is no change in the composition of the clay after it combines with ZnO appreciably; indeed, it still retains its original properties.

Moreover, the peaks of bentonite in the composite were sharper and broader than those of pure bentonite. This is due to the distorted structure of the bentonite crystallites, which results from the support process, increasing the surface area of the material composite. Therefore, when this composite material was used, it had strong adsorption activity.

In addition, the average size of the ZnO crystals in this composite was found to be approximately 20 nm via the Scherrer equation. This value is less than that of pure ZnO, a phenomenon due to the adhesion of ZnO nanoparticles to the bentonite surface. Once such adhesion has occurred, there is no chance for further growth of ZnO particles. These results agree with those of previous research [103], which revealed that the use of a support material can decrease the size of particles and improve their properties.

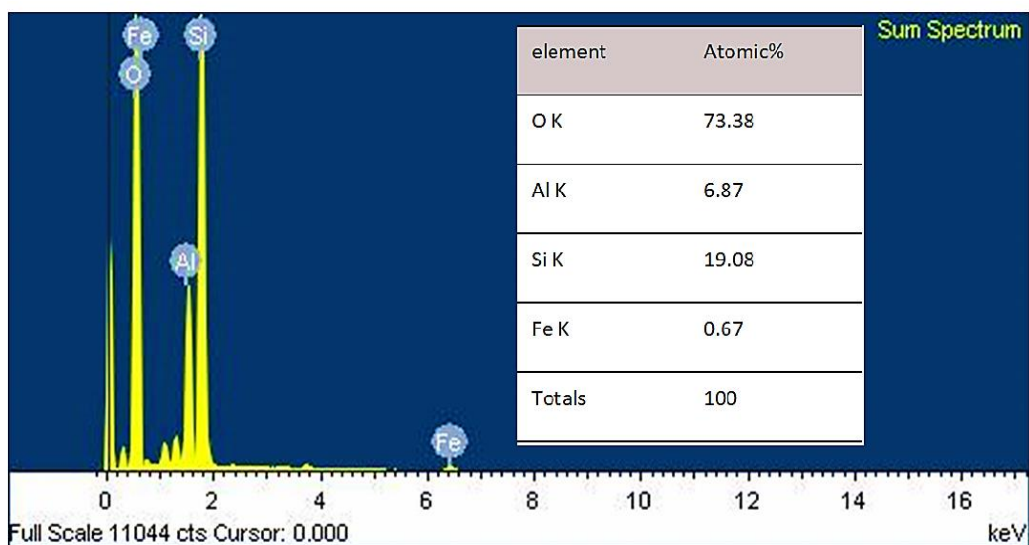
3.1.3 Energy dispersive X-ray (EDX)

EDX analysis is a technique used to determine the elemental composition of materials and measure the proportions of different elements. This approach is beneficial for studying composite materials, as it helps confirm the addition of new elements and assess the material's purity. In this study, EDX was used to analyze both raw bentonite and the ZnO/bentonite composite catalyst to confirm the deposition of ZnO on the surface of bentonite.

The analysis of bentonite revealed major peaks for silicon (Si), oxygen (O), aluminum (Al), and iron (Fe), as shown in Figure 3.5.

Figure 3.5

Shows the X-ray spectrum of a raw bentonite clay sample, with prominent peaks representing the different elements in the sample. The accompanying table shows the percentages of the atomic composition of the elements detected in the sample



The presence of these elements is consistent with the general composition of bentonite, which is mainly composed of clay minerals rich in silica (SiO_2) and alumina (Al_2O_3) with small amounts of iron, which are usually impurities or minor components of bentonite.

Oxygen appears as the highest percentage in the spectrum (73.38%), reflecting the basic composition of bentonite as hydrated aluminum silicate $\text{Al}_2\text{Si}_2\text{O}_5(\text{OH})_4$, where oxygen is bound to other elements. It is followed by silicon at 19.08%, reflecting the silica-rich nature of bentonite, which is the main component of the clay structure.

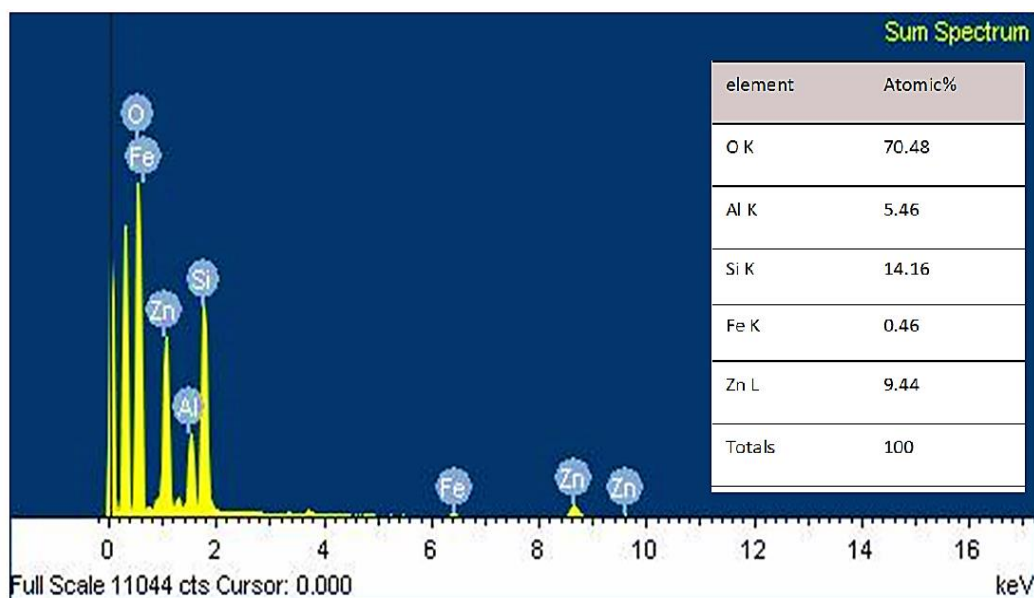
Aluminum (6.87%) indicates the presence of aluminum silicate in the layered structure, whereas a small percentage of iron (0.67%) represents impurities or trace amounts of iron oxides or ferrous metals.

On the other hand, the results of the analysis of the ZnO/bentonite composite catalyst clearly revealed a peak corresponding to zinc (Zn) at 9.44%, which is the main element in ZnO and forms part of the composite. This confirms the successful addition of zinc oxide to the surface of the bentonite.

The oxygen peak is prominently displayed at 70.48% of the atomic composition, indicating a significant percentage of oxygen, which is expected given the nature of zinc oxide (ZnO) and the presence of bentonite, both of which contain oxygen in their composition. Aluminum (Al) is also present at 5.46%, silicon (Si) at 14.16%, and iron (Fe) at a small percentage of 0.46%, reflecting the structure of bentonite and confirming its presence. As shown in Figure 3.6.

Figure 3.6

Shows the X-ray spectrum of a ZnO/bentonite composite sample, with prominent peaks representing the different elements in the sample. The accompanying table shows the percentages of the atomic composition of the elements detected in the sample



A slight decrease in the percentages of silicon, aluminum, oxygen, and iron peaks was observed compared with those of raw bentonite, indicating that zinc oxide partially covers the surface of bentonite.

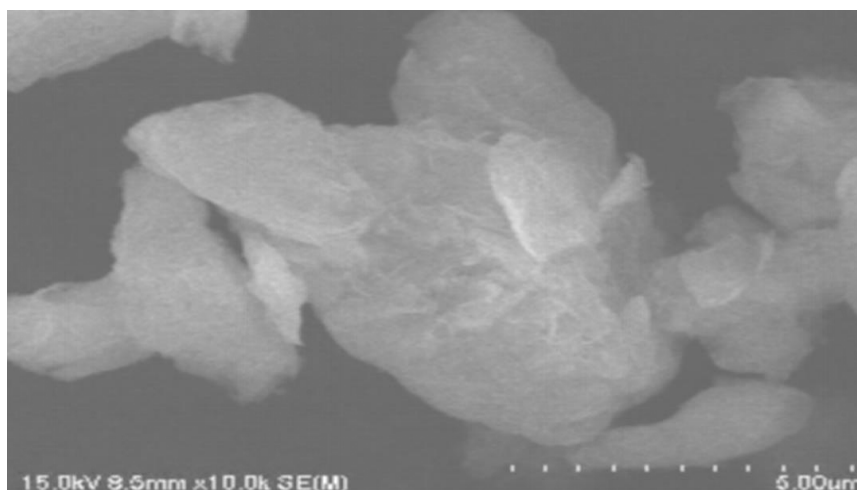
These results indicate the successful deposition of ZnO nanoparticles on the surface of the bentonite. This structural modification is important for enhancing its effectiveness, as it improves its catalytic performance and provides an effective surface for chemical reactions.

3.1.4 Scanning electron microscope (SEM)

The SEM micrographs, at a scale of 5 μm , show the particulate morphology of bentonite clay. The particles are irregularly shaped and flaky, with a plate-like structure common to bentonite clay. The micrographs revealed variations in particle size, with some single flakes and others aggregated into clusters. This also shows that the particle texture is rough, increasing the surface area of the material and supporting its applicability for adsorption processes, as shown in Figure 3.7.

Figure 3.7

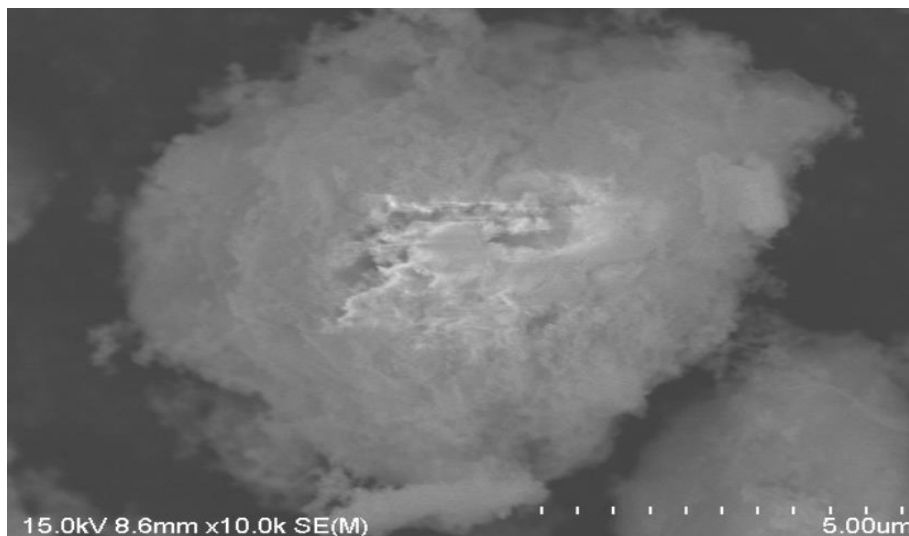
SEM image of the bentonite microflacks



SEM micrographs captured at a scale of 5 μm for the ZnO/bentonite composite indicated the successful incorporation of ZnO nanoparticles into the bentonite microparticles. This showed the ZnO nanoparticles were small, spherical structures that were very well dispersed and attached to the surfaces of the microflakes of the bentonite particles. The bentonite particles provided a substrate that was both rough and irregular, thus allowing for the anchoring of the ZnO nanoparticles. This structural arrangement reflects strong interfacial interactions between the ZnO nanoparticles and the bentonite matrix, which might lead to an improvement in functional properties, such as photocatalytic activity and adsorption ability, as shown in Figure 3.8.

Figure 3.8

SEM image of ZnO/bentonite



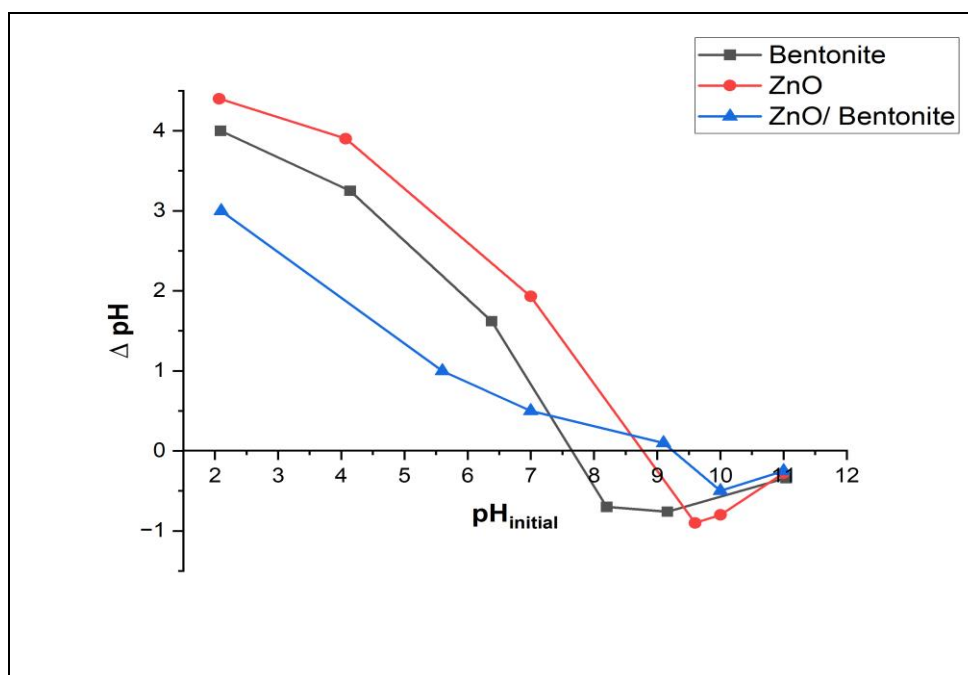
3.1.5 Zero-point charge - ZPC

The point of zero charge (pH_{pzc}) of ZnO, bentonite clay, and the ZnO/bentonite composite was studied to determine the surface properties and electrical charges of these materials under different pH conditions. The study of pH_{pzc} is essential for understanding the adsorption and photodegradation behavior, as it determines at what pH values the surface becomes positive or negative, which affects its interaction with various pollutants. On the basis of this study, the optimum conditions required for using the catalyst to remove tetracycline from water can be determined. Figure 3.9 shows the ΔpH vs. initial pH curves of different solids obtained via the drift method. The results show that the pH_{pzc} of ZnO is approximately 8.8, which means that the ZnO surface has a positive charge in solutions with a pH below 8.8 and a negative charge in solutions with a pH above 8.8.

For bentonite, the pH_{pzc} is estimated to be approximately 7.6, whereas the pH_{pzc} of the ZnO/bentonite composite system is approximately 9.4, indicating that the surface of the composite catalyst is positively charged at pH values below 9.4 and negatively charged at pH values above 9.4. These results will be revisited later when discussing the effects of pH on the adsorption and photodegradation of tetracycline.

Figure 3.9

Plots of ΔpH vs. initial pH measured for ZnO, bentonite clay, and ZnO/bentonite clay. The experiment was performed at 25 °C. Intercepts show values of pH_{pzc} for different solids



3.2 Tetracycline photodegradation study

The absorption of tetracycline was studied via UV–vis spectroscopy. The results showed that tetracycline mainly absorbs in the UV range between 270 nm and 380 nm, with prominent absorption peaks at 275 nm and 356 nm [104]. 356 nm was chosen as the maximum wavelength for the photodegradation experiments. Appendix A5 shows the absorption spectra of the tetracycline solution.

A photodegradation experiment was conducted to study the effect of the presence of the ZnO/bentonite catalyst on the absorption of tetracycline, and the results shown in appendix A6 revealed a gradual decrease in the absorption intensity at 356 nm for tetracycline in the presence of the catalyst. After 90 min, the peak at this wavelength had significantly diminished compared with the initial concentration of tetracycline. This decrease is due to the photoreaction of tetracycline, which is initiated when ZnO supported on bentonite absorbs UV light, leading to the gradual degradation of tetracycline molecules.

Although UV light is effective, its high cost makes the use of sunlight a more economical option. However, since sunlight contains only approximately 5% UV light,

the efficiency of ZnO alone under these conditions is limited. However, this problem has been overcome by supporting ZnO on bentonite, where tetracycline is first adsorbed onto the bentonite surface, which increases the concentration of tetracycline on its surface. This initial adsorption facilitates the subsequent reaction with ZnO, enhancing the efficiency of the photodegradation process even under natural sunlight conditions.

3.2.1 Control experiment results

A series of experiments were conducted to evaluate the effects of both light and the catalyst on the degradation of tetracycline.

The experiments were carried out under three different conditions, where the first experiment included studying the degradation of tetracycline without using catalysts, and the results indicated that no decomposition occurred in the dark. On the other hand, spontaneous photodegradation occurred under light, but this degradation was slow and ineffective at removing tetracycline, as the percentage of removal reached 11% within 60 min of light exposure, as shown in appendix A7. This finding indicates that the degradation of tetracycline requires a long period of time to achieve simple results; therefore, the direct photodegradation of tetracycline by light alone was ignored.

The second experiment included studying the degradation of tetracycline in the absence of light using different types of catalysts, namely, ZnO, bentonite, and ZnO supported on bentonite (ZnO/bentonite).

The results showed that the degradation efficiency in the dark varied depending on the type of catalyst used. In the case of using ZnO alone, limited degradation of tetracycline was observed, as Appendix A8 shows that the percentage of removal of tetracycline reached 9% within 90 minutes, which is (~4 ppm) because ZnO has a very low adsorption capacity, which leads to a decrease in the concentration of tetracycline, but to a very small extent, since ZnO depends mainly on light to stimulate electrons and holes that contribute to the chemical reactions necessary to generate active oxygen species such as hydroxyl radicals (OH^\bullet) and superoxide ($\text{O}_2^{\bullet-}$), which work to break down pollutants. Therefore, the adsorption of tetracycline by ZnO was ignored because of its low absorption rate.

Bentonite alone was observed to be an effective adsorbent for pollutants in the dark because of its large surface area and negative surface charge. This reduces the concentration of pollutants in the aqueous solution without the need for chemical reactions or light. However, its efficiency is limited, as after 90 minutes, the percentage of removal by adsorption on bentonite was only 44%, as shown in appendix A8.

The best period for the adsorption of tetracycline was 30 min because after this time, the adsorption starts to stabilize, indicating that it has reached a steady or equilibrium state. Even though the removal efficiency at 30 min was approximately 40%, the difference in efficiency between 30 and 90 min was not large. Therefore, we chose this time for our experiments because the small increase in efficiency after that was not worth the extra time.

On the other hand, supporting ZnO on bentonite slightly decreased the removal, as Appendix A8 shows that the percentage of removal reached 39% within 90 minutes. The removal rate remains limited because ZnO mainly depends on light to activate its catalytic role; therefore, in the dark, the ability of bentonite to adsorb is more reliant upon removal. In addition, the presence of ZnO on the surface of bentonite reduced the number of active sites required for the reaction, leading to less adsorption of tetracycline.

The readings started to stabilize after 30 min, with a removal efficiency of approximately 35%. The small increase in efficiency after that time shows that extending the adsorption period did not make a large difference in removal, confirming our earlier findings.

The third experiment included studying the degradation of tetracycline in the presence of light to study its effect using the same types of catalysts, where the results revealed a difference in the efficiency of the degradation process depending on the type of catalyst used.

When ZnO was used alone under light, it showed remarkable efficiency as a photocatalyst, as the percentage of removal reached 65% after 60 minutes of irradiation, as shown in appendix A7.

This efficiency is due to the ability of ZnO to absorb light, especially in the ultraviolet range, which leads to the generation of negative electrons and positive holes, which in turn react with water and oxygen molecules to produce active oxygen species such as

free radicals and superoxide, where they are considered highly reactive and capable of breaking down bonds in organic compounds. Thus, these processes contribute to the effective degradation of tetracycline. However, this percentage is considered insufficient to achieve high efficiency in removing tetracycline, as environmental processes usually need higher efficiencies to ensure effective treatment of polluted water.

The results showed that the use of bentonite alone under light is not significantly affected by the presence of light, as it depends on its ability to adsorb pollutants on its surface only and not on chemical or catalytic reactions. The percentage of removal of tetracycline reached 43% within 60 minutes, as shown in appendix A7. This finding is similar to what was obtained when bentonite alone was studied in the dark, indicating that light did not significantly affect its ability to adsorb. Unlike photocatalysts such as ZnO, bentonite does not have the ability to respond to light to cause degradation reactions. Therefore, when bentonite is exposed to light alone, its effectiveness is not significantly improved, limiting its ability to remove pollutants without the presence of a photocatalyst.

In contrast, the results were more positive when the ZnO/bentonite catalyst was used, as the results revealed a significant increase in the degradation rate compared with that with the use of ZnO or bentonite alone. As shown in appendix A7, the percentage of removal reached 87% after 60 minutes of irradiation. This can be explained by the synergistic effect of both bentonite and ZnO, where bentonite acts as an effective adsorbent, adsorbing pollutants onto its surface and increasing the concentration of pollutants near the ZnO particles. Moreover, ZnO acts as a strong photocatalyst, absorbing UV light and generating active free radicals, which in turn react with tetracycline and aid in its degradation. This integration of adsorption by bentonite and photocatalysis by ZnO increases the efficiency of the process, resulting in a significant improvement in the degradation efficiency.

3.2.2 pH effect

pH is an important environmental factor that affects the removal efficiency of tetracycline from water. The effects of different pH values on the degradation of tetracycline via the ZnO/bentonite catalyst were studied, and the results revealed that the removal efficiency of tetracycline varied with pH, indicating its significant effect on the effectiveness of the reaction between tetracycline and the photocatalyst.

The behavior of tetracycline is highly dependent on the pH of the solution, as tetracycline can appear in four different forms, depending on its pKa values, as shown in appendix A9 [105]. In strongly acidic media (pH less than 3.3), tetracycline exists as a positively charged cation ($pK_{a1} = 3.3$), and when the pH is between 3.3 and 7.7, it transforms into the neutrally charged zwitterion form, which carries positive and negative charges ($pK_{a2} = 7.7$), whereas in moderately basic media (pH between 7.7 and 9.7), it exists as a weakly charged negative ion, and at pH values higher than 9.7 ($pK_{a3} = 9.7$), the molecule becomes in its fully negatively charged anionic form, as shown in appendix A10 [106]. These changes in charge directly affect the reactions of tetracycline with the catalyst.

The results revealed that the best removal of tetracycline occurred at basic pH (pH 8.5), where the removal rate of tetracycline reached approximately 87%. This was followed by neutral and moderately acidic pH, where the efficiency was good but less than what was achieved in the basic medium, where the percentage of tetracycline removed was approximately 80% at pH 7.0 and 77% at pH 5.3. At high basic pH or high acidity, the efficiency decreased significantly, reaching 65% at pH 10.1 and 60% at pH 3.0, as shown in appendix A11.

The interaction between tetracycline and the catalyst depends largely on the electrostatic attraction or repulsion between the surface charge of the catalyst and the charge of the tetracycline molecules, which changes according to the pH of the solution. From this perspective, the results obtained can be explained.

For example, under strongly acidic conditions (pH 3.0), tetracycline has a positive charge. Since the pH_{pzc} of the ZnO/bentonite catalyst is 9.4, the surface also has a positive charge in this acidic medium. This similarity in charge between the catalyst surface and the tetracycline molecules results in strong repulsion. As a result, there is a weak interaction between tetracycline and the catalyst, which leads to a decrease in the removal efficiency of tetracycline.

At neutral pH (pH 7.0), tetracycline is a neutral ionic zwitterion. However, ZnO/bentonite has a positive charge because the pH of the solution was lower than the pH_{pzc} of the catalyst. As a result, slight electrostatic repulsion occurs between the catalyst and tetracycline, which slightly reduces the removal rate but still maintains a high overall efficiency.

At pH 5.3, tetracycline exists mainly as a zwitterion with both positive and negative charges; the catalyst surface is also positively charged. As a result, the removal efficiency is reduced because of the slight repulsion between them. In addition, in acidic media, the concentration of OH^- is low, which limits the formation of the hydroxyl radicals ($\cdot\text{OH}$) necessary for the decomposition of tetracycline. Thus, tetracycline cannot appropriately interact with the catalyst, and with time, the efficiency of degrading tetracycline decreases. Compared with pH 7.0, a higher OH^- concentration enhances interactions with the catalyst, leading to improved photocatalytic efficiency.

At pH 8.5, tetracycline is negatively charged, whereas the surface of the ZnO/bentonite catalyst is still positively charged. This difference in charge causes an attraction between the negatively charged tetracycline and the positively charged surface of the catalyst, improving the photodegradation efficiency and thus enhancing the removal rate of tetracycline.

On the other hand, in a strongly basic medium (pH 10.1), tetracycline is completely anionic, and the ZnO/bentonite surface also becomes negatively charged because the pH_{pzc} of the catalyst is exceeded. This negative charge matching between the catalyst surface and the tetracycline molecules leads to significant repulsion. As a result of this repulsion, the interaction between tetracycline and the catalyst becomes weaker, leading to a decrease in the removal efficiency of tetracycline in highly basic media. However, the photodegradation efficiency at pH 10.1 is still greater than that at pH 3.0 because of the abundance of hydroxide ions (OH^-) in the basic medium. These hydroxide ions facilitate the formation of hydroxyl radicals ($\cdot\text{OH}$), which are responsible for degrading tetracycline.

3.2.3 Temperature effect

Temperature is one of the main factors affecting the efficiency of the photodegradation process, as it plays an important role in improving the conditions that support the removal of pollutants. By adjusting the temperature, the reaction rate can be improved, and the activity and stability of the catalyst can be increased, which enhances the effectiveness of photodegradation in removing pollutants.

Different temperatures ranging from 7 to 57 °C were studied to determine their effects on the efficiency of tetracycline removal from water by the ZnO/bentonite catalyst.

The results revealed that the best removal of tetracycline occurred at low temperatures. The tetracycline removal rate reached 89% at 7 °C but decreased to 88% at 15 °C. However, a similar outcome was also obtained at medium temperatures. The tetracycline removal rate reached approximately 87% at 25 °C and 85% at 30 °C. We did not observe a marked difference between the lower and moderate temperatures. This is what made us work at room temperature. On the other hand, at high temperatures, the results were worse, with the removal rate reaching 77% at 57 °C. This temperature had a negative effect on the efficiency of the photodegradation process and thus reduced the ability of the catalyst to remove tetracycline effectively, as shown in appendix A12.

The results were interpreted in terms of the influence of temperature on the reaction rate, catalyst activity, and interaction between pollutants and the catalyst. Together, these factors determine the efficiency of the tetracycline removal process.

The results showed that the catalyst works more efficiently at lower temperatures, especially between 7 and 15 °C. This can be explained by the fact that the catalyst decomposes less and lasts longer at these temperatures and thus successfully catalyzes the reaction. Moreover, the free radicals generated during the photocatalytic process are more stable at lower temperatures. As a result, they remain in the solution for a longer time, increasing their chances of reacting with tetracycline molecules and leading the pollutants to breakdown more effectively. This conclusion highlights the importance of maintaining low temperatures to achieve optimal tetracycline removal through photodegradation.

The reaction was highly efficient at moderate temperatures (25–30 °C). At these temperatures, free radicals such as OH^\bullet and $\text{O}_2^{\bullet-}$ are effectively formed, which interact with tetracycline molecules and increase the efficiency of removal. In addition, the activation energy required to initiate photodegradation is sufficient, ensuring that the reaction occurs effectively. Moderate temperatures also help maintain the catalyst's activity and stability, ensuring its efficient performance throughout the photodegradation process. Although these results are slightly lower than those at even lower temperatures, high efficiency is still achieved.

On the other hand, a decrease in the reaction efficiency was observed at high temperatures (57 °C). This can be explained by the fact that high temperatures can

stimulate the decomposition of active free radicals before they react with tetracycline molecules. In addition, it can damage the catalyst and thus affect its stability, leading to its decomposition, which reduces the overall efficiency of the process. In addition, high temperatures create unwanted reactions and products that may serve as secondary reactions interfering with the primary process, thus reducing the efficiency.

3.2.4 Effect of the amount of ZnO/bentonite catalyst

The quantity of catalyst used is a decisive factor in determining the effectiveness of the photodegradation process in removing pollutants. In this study, different masses of the ZnO/bentonite catalyst were tested to determine the amount that resulted in the most significant rate of tetracycline removal. The amount of catalyst studied ranged from 0.05 to 0.5 g.

The results demonstrated that the highest efficiency for tetracycline removal was when 0.1 g of ZnO/bentonite catalyst was used, with the removal rate reaching 87%. On the other hand, adding 0.05 g of catalyst led to a lower removal rate of 85%. Moreover, the removal rate of 0.2 g of the catalyst was slightly lower than that of 0.1 g, with an 83% removal rate. As the amount of catalyst increased from 0.3 to 0.5 g, no significant improvement in removal rates occurred, and the removal rates remained relatively constant between 77% and 79%, as shown in Appendix A13. This suggests that beyond 0.3 g, adding more catalyst becomes ineffective, meaning that the maximum possible effect has been reached, where increasing the amount of catalyst no longer results in any further improvement in removal efficiency.

The number of active sites on the catalyst explains these results. When the amount of ZnO/bentonite catalyst was 0.1 g, there were adequate active sites on their surface, which ensured an effective reaction with tetracycline and, consequently, better degradation.

At 0.05 g of the catalyst, its lower amount still enabled effective degradation of tetracycline, but the efficiency decreased slightly, suggesting that the number of active sites available was too low to allow full utilization of the photocatalytic activity.

When the catalyst amount was 0.2 g, there was a slight decrease in the percentage of tetracycline removed. This minor decline may be attributed to the reduction in light penetration when the catalyst loading exceeds the optimal level, leading to reduced

activation of ZnO and a slight decrease in the generation of reactive species. However, the performance at 0.2 g remains relatively comparable to the optimal value, indicating its potential viability for effective tetracycline removal.

When the catalyst amount increased from 0.3 to 0.5 g, the removal rate reached a constant value, with no significant improvement in efficiency. This suggests that excessive catalyst loading does not enhance the degradation process and may, in fact, hinder it. The reduced efficiency at higher catalyst amounts can be attributed to the agglomeration and stacking of catalyst particles, which decrease the available active surface area by making some catalytic sites inaccessible. Additionally, the increased catalyst concentration can cause light blocking, which limits light penetration and reduces photoactivation of ZnO. Together, these effects hinder the formation of the reactive species necessary for tetracycline degradation.

3.2.5 Effect of the tetracycline concentration

The results showed that the tetracycline removal efficiency was highest at low concentrations, specifically 10, 20, and 30 ppm, where the percentage of removal reached 98%, 97%, and 95%, respectively. The catalyst removed almost all of the tetracycline present, resulting in very high efficiency. However, since the initial tetracycline concentration was very small, the total amount of tetracycline removed by the catalyst was very small: approximately 9.8 mg/L at 10 ppm, 19 mg/L at 20 ppm, and 29 mg/L at 30 ppm, as shown in appendix A14.

In contrast, when the concentration was increased to 40 ppm, the removal rate decreased to 87%, but the total amount of tetracycline removed increased significantly to approximately 35 mg/L. At 50 ppm, although the efficiency decreased to 72%, the total amount removed was 36 mg/L, which is almost the same as that at 40 ppm. This finding indicates that the amount of tetracycline starts to stabilize after reaching a concentration of 40 ppm, as shown in appendix A14.

This can be explained by the fact that when tetracycline is present in small amounts, such as 10, 20, and 30 ppm, the catalyst works very efficiently and removes many pollutants as a percentage, but since the initial concentration is very small and the number of tetracycline molecules available in the solution is low, the amount of tetracycline removed generally remains low, even if the removal rate is high.

At a concentration of 40 ppm, the amount of tetracycline removed increases because it allows many tetracycline molecules to interact with the active sites on the surface of this catalyst in addition to interacting effectively with free radicals. This explains why although the removal efficiency is greater at lower concentrations, the total amount of tetracycline removed increases with increasing concentration until it reaches its peak at 40 ppm.

On the other hand, at a concentration of 50 ppm, although the amount of tetracycline removed was slightly greater, it was small and insignificantly increased, and the removal efficiency decreased significantly. This is because the excess tetracycline molecules block the light needed for an effective reaction; thus, less light is available to activate the catalyst. In addition, excess tetracycline molecules accumulate on the surface of the catalyst, leading to saturation, thus reducing its ability to effectively remove pollutants. Consequently, the photodegradation process is slower and less efficient.

For this reason, we chose 40 ppm as a suitable and optimal concentration for the rest of our experiments, as it provides a better way to evaluate catalyst performance and achieves a balance between removal efficiency and the total amount of pollutants removed. Furthermore, we confirmed 40 ppm as the optimal concentration in the kinetic results section, where the kinetic parameters further confirmed its superior performance over other concentrations.

3.2.6 Effect of oxygen

Oxygen has a significant effect on the efficiency of the photodegradation process. It plays a key role in the production of free radicals that interact directly with tetracycline molecules, making them decompose easily.

The results revealed efficient and remarkable degradation of tetracycline with enough oxygen, where the percentage of removal reached 95%, as shown in Appendix A15.

One of the most important reasons is that when there is oxygen in the reaction system, it serves as an electron acceptor. This mechanism, described by equation (1.2), makes it easier for electrons released from the light-exposed catalyst surface to undergo reduction reactions rather than be lost. Oxygen radicals such as ($O_2^{\cdot-}$) are generated during this process. These highly active oxygen species breakdown tetracycline molecules into smaller parts, thus accelerating decomposition and increasing the removal rate.



A sufficient level of oxygen means that there is a lower chance of electrons combining with positive holes; therefore, this ensures that more electrons remain free to produce reactive oxygen species, enhancing the photodegradation reaction.

3.2.6 Effect of carbon dioxide

The photodegradation process is significantly influenced by CO₂. This is because its presence in the reaction medium has negative effects, such as altering the pH of the solution. In addition, CO₂ affects the absorption of light by the catalyst, which is a crucial initial step for photodegradation. Together, these effects can diminish the generation of radical species that are necessary for the breakdown of pollutants, lowering the efficiency of the process as a whole.

The results showed that the presence of CO₂ markedly decreased the tetracycline degradation rate to 50%, as shown in appendix A16. This negative effect occurs for several reasons.

One of the main factors is the effect of CO₂ on the pH of the reaction medium. CO₂ dissolves in water to form carbonic acid (H₂CO₃), which leads to a decrease in pH. This decrease affects the efficiency of the catalyst. As previously mentioned, the catalyst works best within a basic pH range, as the efficiency in acidic media decreases due to the repulsion of surface charges between the catalyst and tetracycline. As a result, the chances of the contaminant binding to the catalyst decrease, and the reaction efficiency decreases.

In addition, CO₂ reacts with free radicals such as [•]OH, which oxidize pollutants and thus decompose them. As a result, (HCO₃⁻) and (CO₃²⁻) ions are formed rather than destroying the pollutant, as shown in equations (3.3) and (3.4). This reduces the number of active radicals available for decomposing tetracycline and makes the process less effective.



Moreover, CO₂ forms a gaseous sheet covering the surface of the catalyst, thus blocking it from light. This decreases the amount of energy absorbed by the catalyst and thus

reduces the activation of the electrons and holes needed to create active species. As a result, the efficiency of the photodegradation process decreases.

3.3 Kinetics of tetracycline photodegradation

The kinetics of photodegradation must be understood to determine how well the catalyst removes pollutants and to determine the optimal conditions for the reaction. This process involves many factors, such as the quantity of catalyst, pollutant concentration, pH of the solution, temperature and other factors, all of which combine to affect the reaction rate and overall efficiency of the process. To gain a clearer understanding of these kinetics, various analytical methods and techniques have been employed to measure the effectiveness of the catalyst in removing pollutants. The basic concepts used to study photodegradation kinetics include the turnover number (TON), turnover frequency (TOF), quantum yield (Q.Y), and number of degraded molecules.

TON refers to the number of molecules that are decomposed by a single unit of the catalyst. As shown in equation (3.5) [107]. If the TON value is high, the catalyst has great efficiency in eliminating large numbers of pollutant molecules.

$$\text{TON} = \frac{\text{Number of moles of reacted contaminant}}{\text{Number of moles of catalyst}} \quad (3.5)$$

The TOF is a measure of how rapidly and effectively a molecule decomposes. where it refers to the number of reactions that occur at each active site per time unit. As shown in equation (3.6) [107]. Generally, catalysts with high TOFs are considered better because they reduce the time needed for a reaction and increase the number of removed pollutants.

$$\text{TOF} = \frac{\text{TON}}{\text{Time (min)}} \quad (3.6)$$

Q.Y expresses the number of molecules that are degraded per UV photon falling on the catalyst. As shown in equation (3.7), [107]. This efficiency indicates the ability of the catalyst to convert light energy into chemical energy.

An increase in Q.Y means that the catalyst uses light more effectively to remove pollutants.

$$Q.Y = \frac{\text{Number of reacted molecules}}{\text{Number of incident light}} \quad (3.7)$$

The number of degraded molecules is one of the main criteria used to measure the effectiveness of the catalyst in removing pollutants, where the number of pollutant molecules that have been degraded and broken down into harmless products by the catalyst was determined via equation (3.8) [107]. where ΔC is the change in pollutant concentration (mol/L), V is the solution volume (L), N_A is Avogadro's number ($6.022 \times 10^{23} \text{ mol}^{-1}$), and M is the molar mass of the pollutant (g/mol).

$$\text{Number of Degraded Molecules} = \frac{\Delta C \times V \times N_A}{M} \quad (3.8)$$

Kinetics were calculated to understand the effects of different factors on the photodegradation process on the basis of the previously mentioned parameters. The effects of pollutant concentration, catalyst amount, pH, temperature, and the presence of oxygen and carbon dioxide on the efficiency of the process were determined, as shown in Tables 3.1, 3.2, and 3.3.

The results showed that these factors directly affect the reaction rates and removal efficiency. The increasing values of the kinetic parameters clearly indicate increased photodegradation efficiency, reflecting the positive effect of the optimum conditions on the performance of the process and enhancing its effectiveness.

The concentration of the pollutant significantly affected the photodegradation process. When the concentration of tetracycline was increased to 40 ppm, an improvement in the values of TON, TOF and Q.Y was observed, reflecting an increase in the number of degraded molecules. However, when the concentration was increased to 50 ppm, the values of TON and TOF were greater, although the removal rate was lower than that at a concentration of 40 ppm. This can be explained by the fact that increasing the concentration enhances the interaction of the catalyst with the pollutants, leading to an improvement in the kinetic parameters, such as TON, TOF and Q.Y, but with increasing concentration, saturation occurs at the catalyst sites, leading to a decrease in the efficiency of pollutant removal, despite the improvement in these values.

For the amount of catalyst, there was an increase in the number of degraded molecules, which was positively reflected in the values of the kinetic parameters, such as TON, TOF and Q.Y. This increase indicates an improvement in the efficiency of photodegradation. However, when the amount of catalyst was increased to greater than 0.1 g, the efficiency began to decrease.

Table 3.1

Effects of the TC concentration and catalyst amount on the kinetic parameters of photodegradation

Effect of TC concentration					
Tetracycline (ppm)	%Degradation	Degraded Molecules (10^{-3})	TON (10^{-5})	TOF (min^{-1})	Q.Y (10^{-2})
$(10^{18}$ (molecule/photon))					
10	98%	1.328	2.991	3.323	0.39
20	97%	2.575	5.798	6.443	0.76
30	95%	3.930	8.850	9.834	1.16
40	87%	4.743	10.681	11.870	1.40
50	72%	4.879	10.987	12.210	1.44
Effect of catalyst amount					
Catalyst amount (g)	% Degradation	Degraded Molecules (10^{18})	TON(10^{-3})	TOF(10^{-5})	Q.Y(min^{-1})
$(10^{-2})(\text{molecule/photon})$					
0.05	85%	4.624	10.413	11.567	1.37
0.1	87%	4.738	10.669	11.857	1.40
0.2	83%	4.481	10.090	11.211	1.32
0.3	79%	4.283	9.645	10.717	1.27
0.4	78%	4.230	9.526	10.584	1.25
0.5	77%	4.147	9.339	10.376	1.23

pH plays an important role in the efficiency of the photodegradation process, with a basic medium providing the best conditions, as shown by the high values of (TON), (TOF), and (Q.Y). Lower temperatures also helped improve the reaction rate and efficiency, as reflected by the increased values of (TON), (TOF), and (Q.Y). However, very high temperatures negatively impact the efficiency.

Table 3.2*Effects of temperature and pH on the kinetic parameters of photodegradation*

Effect of temperature					
Temperature (°C) (10 ⁻³)(molecule/photon)	%Degradation	Degraded Molecules(10 ⁻³)	TON (10 ⁻⁵)	TOF (10 ⁻⁵)	Q.Y) (min ⁻¹)
7	89%	4.841	10.901	12.112	1.43
15	88%	4.759	10.718	11.909	1.41
25	87%	4.689	10.560	11.733	1.39
30	85%	4.597	10.352	11.502	1.36
57	77%	4.174	9.340	10.444	1.23
Effect of pH					
pH (10 ⁻²)(molecule/photon)	% Degradation	Degraded Molecules (10 ¹⁸)	TON (10 ⁻³)	TOF (10 ⁻⁵)	Q.Y (min ⁻¹)
.03	60%	3.252	7.324	8.138	0.96
5.3	77%	4.174	9.340	10.444	1.23
8.5	87%	4.716	10.620	11.800	1.39
7.0	80%	4.337	9.766	10.851	1.28
10.1	65%	3.523	7.935	8.816	1.04

Oxygen improved the reaction by increasing free radical production, increasing the values of kinetic parameters such as the Q.Y. and TON. In contrast, carbon dioxide reduced efficiency by consuming free radicals, leading to lower TON and TOF values, indicating a reduced photodegradation efficiency.

Table 3.3*Effects of oxygen and carbon dioxide on the kinetic parameters of photodegradation*

Effect of oxygen					
Oxygen presence (10 ⁻³)(molecule/photon)	%Degradation	Degraded Molecules(10 ¹⁸)	TON (10 ⁻³)	TOF (10 ⁻⁵)	Q.Y) (min ⁻¹)
Present	95%	5.150	11.597	12.885	1.52
Effect of carbon dioxide					
CO2 presence (10 ⁻²)(molecule/photon)	% Degradation	Degraded Molecules (10 ¹⁸)	TON (10 ⁻³)	TOF (10 ⁻⁵)	Q.Y (min ⁻¹)
.03	50%	2.710	6.1034	6.782	0.80

3.4 Activation energy

The activation energy is a fundamental concept for understanding chemical processes. It represents the energy needed for molecules to reach the transition state. In other words, it is the minimum energy that is required to start the reaction.

The rate of a chemical reaction depends on the energy level of its reactant molecules. If their energy is less than the activation energy, no reaction will occur; however, the reaction will start if the reactants have energy equal to or greater than the activation energy.

Equation (3.9) of the Arrhenius equation describes the relationships among the rate of a reaction, the temperature, and the activation energy [108]. This formula also provides a tool for analyzing how changing reaction conditions, such as temperature, might speed up or slow down subsequent chemical reactions and, thus, how the nature of a system affects the reaction rate.

$$K = A \times e^{-E_a/RT} \quad (3.9)$$

where K is the rate constant, A represents the Arrhenius coefficient, which is a frequency factor that reflects the number of successful collisions between molecules, e is the natural base of logarithms (approximately 2.718), E_a is the activation energy (J/mol), and R is the universal gas constant, which has a value of 8.314 J/mol. K), T is the absolute temperature (in Kelvin).

This formula can be linearized via the natural logarithm, as shown in equation (3.10) [108]:

$$\ln(K) = \ln(A) - \frac{E_a}{R} \times \frac{1}{T} \quad (3.10)$$

The relationship between $\ln(k)$ and $\frac{1}{T}$ was plotted to determine the activation energy E_a .

We obtained a linear form, as shown in appendix A17, which allows the value of E_a to be calculated on the basis of the line slope.

The Arrhenius equation was used to determine the effects of various temperatures on the removal rate of tetracycline. The calculations revealed that the activation energy was 5

kJ/mol. This means that the reaction happens quickly and easily. Therefore, there is no need for high energy to initiate the reaction, which explains why the ZnO/bentonite catalyst is functional efficiently under low- to moderate-temperature conditions. Interestingly, while higher temperatures may increase the reaction rate, they also lead to negative effects. For example, active radicals can be degraded, or unwanted side reactions can occur, thus reducing overall efficiency. This phenomenon tallies with what was found in an earlier discussion of temperature effects, where the efficiency of the catalyst was emphasized at lower and moderate temperatures by a low activation energy value, indicating its efficiency.

Furthermore, because the activation energy is very low, the adsorption process at the surface of bentonite involves physical adsorption. This means that tetracycline interacts with the surface via weak forces such as van der Waals forces.

This rapid adsorption type requires little energy, making it particularly suitable for environmental applications such as removing tetracycline from water. In addition, the pollutants can be easily separated from the adsorbent, and the catalyst remains reusable, as this process does not significantly damage it or alter its properties. This is important, for example, with fast and efficient pollutant removal, making it cost-effective and suitable under different conditions.

3.5 Order of the reaction

The reaction order explains how chemical reactions can be strongly affected by changes in reactant concentrations, such as those of catalysts or pollutants. By understanding this concept, we gain deeper insight into the reaction mechanism, determine the optimal conditions, and ultimately, improve the efficiency.

The reaction order is the slope obtained by plotting the natural logarithm of the reaction rate $\ln(\text{rate})$ against the natural logarithm of the concentration of reactants $\ln(\text{concentration})$.

The reaction order was determined via experimental data obtained from tetracycline removal experiments with a ZnO/bentonite catalyst under two variables:

- Variation in the tetracycline concentration.
- Variation in the amount of ZnO/bentonite catalyst. The amount of catalyst was

considered equivalent to its concentration because the reaction volume was constant.

The general law for the rate of reaction is given in equation (3.11) [109]:

$$\text{Rate} = K [\text{tetracycline}]^x [\text{catalyst}]^y \quad (3.11)$$

The natural logarithm is used, as shown in equation (3.12) [108]:

$$\ln (\text{Rate}) = \ln (K) + x \ln ([\text{tetracycline}]) + y \ln ([\text{catalyst}]) \quad (3.12)$$

(x) The order of reaction with respect to the tetracycline concentration. (y) is the reaction order with respect to the catalyst quantity used.

The order of the reaction was calculated as the slope of the straight line resulting from the relationship between $\ln (\text{rate})$ and $\ln ([\text{tetracycline}])$ or $\ln ([\text{catalyst}])$. Importantly, when plotting the relationship between $\ln (\text{rate})$ and $\ln ([\text{tetracycline}])$, $\ln (k)$ and $\ln ([\text{catalyst}])$ are considered constant, and the opposite is true when plotting with catalyst amount.

For the tetracycline concentration. When the tetracycline concentration was changed and $\ln (\text{rate})$ was plotted versus $\ln ([\text{tetracycline}])$, the slope was found to be 0.2, as shown in appendix A18.

This indicates that the reaction rate is weakly dependent on the pollutant concentration, as increasing the concentration leads to an increase in the reaction rate and efficiency. This is consistent with the previous results in terms of the effect of the pollutant concentration. Increasing the pollutant concentration leads to an improvement in efficiency up to a concentration of 40 ppm, where the efficiency is at its peak at this concentration. After that, the efficiency starts to decrease at higher concentrations.

For the catalyst amount. When the catalyst amount was changed and $\ln (\text{rate})$ was plotted versus $\ln ([\text{catalyst}])$, the slope was found to be 0.1, as shown in appendix A19.

This indicates that the effect of the amount of catalyst on the reaction rate is relatively weak. The reaction rate is almost independent of the catalyst amount beyond a certain limit, which means that increasing the catalyst amount after this limit does not significantly affect the reaction rate. This is compatible with the results of the study of the effect of catalyst amount, where it was found that above 0.1 g, the efficiency

decreased very slightly, which is consistent with the result that increasing the catalyst amount beyond this amount did not significantly affect the reaction efficiency. These results indicate that the system works effectively in removing tetracycline with high efficiency without the need for large amounts of catalyst, making it suitable for environmental applications, such as water treatment with high efficiency and low cost.

3.6 Recovery and reuse of the ZnO/bentonite catalyst

One of the reasons why the recovery of ZnO nanoparticles is complex is their small nanosize; it is difficult to use traditional methods such as filtration and precipitation for separation. However, combining ZnO with bentonite solves this problem by supporting zinc oxide on bentonite, which allows the catalyst to separate from the reaction medium via low-cost techniques. This makes ZnO/bentonite a practical environmental catalyst with high efficiency.

The effectiveness of tetracycline removal was tested after the catalyst had been used five times. The first time the catalyst was used, 87.5% of all the tetracycline was removed. Up to the fifth cycle, the percentage gradually decreased to 77%, as shown in appendix A20. This slight decrease was mainly the result of weight loss in the separation and reuse processes rather than any significant changes in the catalyst composition or structure. However, the catalyst maintained a high-efficiency level over five cycles, indicating excellent stability.

3.7 Tetracycline complete mineralization confirmation

The photocatalytic activity of ZnO/bentonite in completely breaking down tetracycline under simulated sunlight was tested. Different techniques were used to observe the reaction.

The results revealed that nearly all the compounds broke down when a solution with a concentration of 40 ppm tetracycline was used with 0.1 g of ZnO/bentonite and irradiated with light for 180 minutes.

In Table 3.4, the results show a steady decline in the content of the compound, with a percentage of elimination of at least 95% on the basis of UV analysis. The absorption peak for the tetracycline spectrum decreased until it disappeared, indicating that the bonds were broken down, leading to a reduction in the concentration of tetracycline. As shown in appendix A21.

HPLC analysis also revealed new peaks indicating the primary decomposition products of tetracycline, indicating that the reaction was not just a slight modification in the structure of the tetracycline but rather involved oxidation and decomposition of the molecule. Over time, these peaks gradually faded until they disappeared completely by the end of the reaction period, with a percentage of removal of approximately 98%. This confirms that the primary decomposition products have been broken down and converted into simpler inorganic compounds, reflecting the complete decomposition of the original compound and its parts.

Table 3.4

Confirmation of complete mineralization of tetracycline by ZnO/bentonite-catalyzed photodegradation. The reaction was conducted with TC (100.0 mL, 40 ppm) and 0.1 g of ZnO/bentonite at pH ~8.5 at 25 °C

Time of irradiation (min)	% TC removal	
	UV-Vis	HPLC
0	0	0
30	40	45
60	59	72
90	87	90
120	92	93
150	93	95

FT-IR spectroscopy (also known as Fourier transform infrared spectroscopy) is a powerful analytical tool for monitoring the progress of tetracycline decomposition.

The spectrum shows different characteristic peaks of the tetracycline compound before the reaction, and these peaks reflect the basic functional groups, as shown in appendix A22. For example, the peak at 2978.5 cm^{-1} signals a stretching vibration of the (C-H) bond in saturated hydrocarbon groups. This indicates that hydrogen molecules are attached to the carbon in the compound structure, which is characteristic of organic compounds. In addition, there is a peak at 3400 cm^{-1} for vibrations of the hydroxyl group (OH), which indicates the polarity of this compound.

The characteristic peak at 1669 cm^{-1} is caused by stretching vibrations of the carbonyl bond (C=O), a major functional

On the other hand, the peak at 1582.3 cm^{-1} corresponds to the stretching vibrations of a (C=C) bond of a nonaromatic ring. This double bond shows the diversity of the tetracycline structure.

The peak at 1615 cm^{-1} is associated with the stretching vibrations of a (C=C) bond that forms part of the aromatic rings. This peak is significant for tetracycline because it reflects its stability and plays a role in its physical and chemical properties.

The peak at 1227.4 cm^{-1} corresponds to the stretching vibrations of the (C–N) bond, indicating that amino groups are present. The peak at 1455.9 cm^{-1} is attributed to the bending vibrations of the (C-H) group.

The FT-IR spectrum of the bentonite-supported ZnO catalyst showed a characteristic peak corresponding to the main functional group of the structure, as shown in appendix A23. The most prominent peak, which is the peak at 1014 cm^{-1} , is assigned to the stretching vibrations of the Si-O-Si bond, a distinct characteristic of clay bentonite. This denotes the silicate-containing layered structure of bentonite, which is one of the primary components of the catalyst.

As tetracycline decomposition begins, the tetracycline peaks gradually disappear. These peaks were evident in the tetracycline compound before the reaction, and over time, a gradual decrease in the intensity of these peaks was observed. By the 180th minute, these peaks completely disappeared, indicating the breaking of the basic functional bonds in the molecule and its transformation into inorganic products. The characteristic peak at 1014 cm^{-1} of the catalyst remained constant, confirming its stability and that it did not undergo any chemical changes during the reaction. As shown in appendixes (A24, A25, and A26).

This performance is attributed to the ability of bentonite to effectively adsorb tetracycline molecules, keeping them close to the ZnO surface rich in active radicals. ZnO is activated under light to generate hydroxyl radicals, which react with tetracycline, breaking its chemical bonds and fully decomposing it into harmless products.

These results show that the ZnO/bentonite system is a powerful and eco-friendly solution for the degradation of persistent organic pollutants. This approach has great potential for effectively and sustainably treating water contaminated with antibiotics.

3.8 Conclusion

In this study, ZnO/bentonite composite was prepared using the precipitation method to enhance the efficiency of ZnO in removing tetracycline. The results showed that combining ZnO with bentonite improved the physical and chemical properties of the catalyst, leading to higher photocatalytic performance under light exposure. The best efficiency was achieved at moderate temperatures and basic pH levels.

The optimal catalyst amount was found to be 0.1 g, while the best tetracycline concentration was 40 ppm, which demonstrated that maintaining a balance in quantity and concentration is crucial for effective results. Adding oxygen significantly accelerated the reaction by increasing the generation of free radicals, whereas carbon dioxide had a negative impact due to its interaction with these radicals.

The low activation energy indicated that the reaction required low energy to start, and confirmed that adsorption on bentonite surface was physical, allowing for easy catalyst recovery and reuse. The reaction order was determined to be 0.2 for tetracycline concentration and 0.1 for catalyst concentration, indicating minimal reliance on the reactants concentration, which contributed to the stability and efficiency of the catalyst.

In addition, the complete degradation of tetracycline under optimal conditions was confirmed, emphasizing the high efficiency of the catalyst in breaking down the compound into inorganic harmless byproducts.

Overall, the study demonstrated that ZnO/bentonite is not only highly efficient but also sustainable and reusable, making it an excellent option for pollutant treatment, particularly for antibiotics, such as tetracycline.

3.9 Recommendations for future work

1. Tetracycline levels in drinking water in Palestine should be measured to assess its environmental risks and better understand the prevalence of this problem.
2. The effects of organic pollutants caused by the war in Gaza, including chemicals from bombings such as heavy metals and harmful organic compounds, which could contaminate groundwater and surface water, should be studied. Therefore, it is recommended to use photodegradation technique with ZnO/bentonite to treat these pollutants.
3. A ZnO/bentonite water treatment system should be designed for developing countries and areas with limited water resources, which includes simple, low-cost units that use solar energy to drive photocatalytic reactions for purifying water contaminated with tetracycline
4. Advanced analytical techniques such as BET (Brunauer-Emmett-Teller) and XPS (X-ray Photoelectron Spectroscopy) should be used to examine the surface properties and chemical composition, helping to enhance the understanding of the adsorption process and photodegradation reactions.
5. The effectiveness of ZnO/bentonite catalyst in removing other pollutants, such as other types of antibiotics and persistent organic compounds, should be determined to expand its range of environmental application.
6. The effects of different environmental conditions (such as the presence of other pollutants or heavy metal ions) on the removal efficiency of tetracycline, should be studied to improve performance in natural environments.
7. The potential environmental impact of the presence of ZnO nanoparticles in water, which may arise from the use of the catalyst, should be evaluated to ensure the design of environmentally safe materials.
8. The by-products resulting from tetracycline degradation should be analyzed using advanced analytical techniques such as GC–MS, to precisely understand the reaction mechanism.
9. The effect of using natural sunlight on tetracycline removal should be studied, and the photodegradation efficiency should be compared when using natural light instead of artificial light, to improve the effectiveness of catalyst application under real-world conditions.

10. An economic and technical evaluation should be performed by conducting a comprehensive economic feasibility study to evaluate the cost of producing ZnO/bentonite compared with other catalysts while studying the possibility of large-scale manufacturing.

List of Abbreviations

Abbreviation	Meaning
a.u	Arbitrary units
A	Arrhenius coefficient
[A]	Concentration of compound A
A•	Radical of compound A
BET	Brunauer–Emmett–Teller
ΔC	Change in pollutant concentration (mol/L)
E _a	Activation energy
e ⁻	electron
eV	Electron volts
EDX	Energy-dispersive X-ray spectroscopy
FT-IR	Fourier-Transform Infrared Spectroscopy
GC–MS	Gas Chromatography–Mass Spectrometry
HPLC	High-Performance Liquid Chromatography
K	Rate constant
min	minute
M	Molar mass of the pollutant (g/mol)
N _A	Avogadro's number ($6.022 \times 10^{23} \text{ mol}^{-1}$)
pKa	Acid Dissociation Constant
PZC	Zero point charge
Q.Y	Quantum Yield
rpm	Round per minute
R	Universal gas constant (8.314 J/mol.K)
SEM	Scanning electron microscopy
TC	Tetracycline
TON	Turnover Number
TOF	Turnover Frequency
T	Absolute temperature (Kelvin)
UV–Vis	Ultraviolet–Visible
V	Solution volume (L)
XRD	X-ray diffraction
XPS	X-ray Photoelectron Spectroscopy
(x)	Reaction order with respect to the concentration of the tetracycline
(y)	Reaction order with respect to the concentration of catalyst

References

1. Shiklomanov IA, Rodda JC. World water resources at the beginning of the twenty-first century: Cambridge University Press; 2003.
2. Mishra RK. Fresh water availability and its global challenge. *British Journal of Multidisciplinary and Advanced Studies*. 2023;4(3):1-78.
3. Meedzan NL, Nicholas PK, Breakey S, Corless IB. Access to Clean Water and the Impact on Global Health: An Interview With Gary White, CEO and Cofounder, Water.org. *Mathematics for Health Professionals*. 1977:123.
4. Martínez-Santos P. Does 91% of the world's population really have "sustainable access to safe drinking water"? *International Journal of Water Resources Development*. 2017;33(4):514-33.
5. Ahamad A, Madhav S, Singh AK, Kumar A, Singh P. Types of water pollutants: conventional and emerging. *Sensors in water pollutants monitoring: Role of material*. 2020:21-41.
6. Ritter KS, Paul Sibley, Ken Hall, Patricia Keen, Gevan Mattu, Beth Linton, Len. Sources, pathways, and relative risks of contaminants in surface water and groundwater: a perspective prepared for the Walkerton inquiry. *Journal of Toxicology and Environmental Health Part A*. 2002;65(1):1-142.
7. Organization WH. Water for health: taking charge. World Health Organization (WHO); 2001.
8. An M, Fan L, Huang J, Yang W, Wu H, Wang X, et al. The gap of water supply—Demand and its driving factors: From water footprint view in Huaihe River Basin. *Plos one*. 2021;16(3):e0247604.
9. Ahmad A, Azam T. Water purification technologies. *Bottled and Packaged Water*: Elsevier; 2019. p. 83-120.
10. Tripathi AK, Pandey SN. Water pollution: APH Publishing; 2009.
11. Dwivedi AK. Researches in water pollution: A review. *International Research*

- Journal of Natural and Applied Sciences. 2017;4(1):118-42.
12. Viman OV, Oroian I, Fleşeriu A. Types of water pollution: point source and nonpoint source. *Aquaculture, Aquarium, Conservation & Legislation*. 2010;3(5):393-7.
 13. Singh J, Yadav P, Pal AK, Mishra V. Water pollutants: Origin and status. *Sensors in water pollutants monitoring: Role of material*. 2020:5-20.
 14. Brusseau M, Artiola J. Chemical contaminants. *Environmental and pollution science*: Elsevier; 2019. p. 175-90.
 15. Sharma S, Bhattacharya A. Drinking water contamination and treatment techniques. *Applied water science*. 2017;7(3):1043-67.
 16. Walworth J, Pepper I. Physical contaminants. *Environmental and Pollution Science*: Elsevier; 2019. p. 163-73.
 17. Bashir I, Lone FA, Bhat RA, Mir SA, Dar ZA, Dar SA. Concerns and threats of contamination on aquatic ecosystems. *Bioremediation and biotechnology: sustainable approaches to pollution degradation*. 2020:1-26.
 18. Hill DD, Owens WE, Tchounwou PB. Impact of animal waste application on runoff water quality in field experimental plots. *International journal of environmental research and public health*. 2005;2(2):314-21.
 19. Zahoor I, Mushtaq A. Water pollution from agricultural activities: A critical global review. *Int J Chem Biochem Sci*. 2023;23(1):164-76.
 20. Ahmed J, Thakur A, Goyal A. Industrial wastewater and its toxic effects. 2021.
 21. Dutta D, Arya S, Kumar S. Industrial wastewater treatment: Current trends, bottlenecks, and best practices. *Chemosphere*. 2021;285: 131245.
 22. Co-Operation OfE, Development. *Pharmaceutical Residues in Freshwater: Hazards and Policy Responses*: IWA Publishing; 2020.
 23. Fernandes JP, Almeida CMR, Salgado MA, Carvalho MF, Mucha AP.

- Pharmaceutical compounds in aquatic environments—occurrence, fate and bioremediation prospective. *Toxics*. 2021;9(10):257.
24. Polianciuc SI, Gurzău AE, Kiss B, Ștefan MG, Loghin F. Antibiotics in the environment: causes and consequences. *Medicine and pharmacy reports*. 2020;93(3):231.
 25. Rogowska J, Zimmermann A. Household pharmaceutical waste disposal as a global problem—a review. *International journal of environmental research and public health*. 2022;19(23):15798.
 26. Barathe P, Kaur K, Reddy S, Shriram V, Kumar V. Antibiotic pollution and associated antimicrobial resistance in the environment. *Journal of Hazardous Materials Letters*. 2024:100105.
 27. Murray CJ, Ikuta KS, Sharara F, Swetschinski L, Aguilar GR, Gray A, et al. Global burden of bacterial antimicrobial resistance in 2019: a systematic analysis. *The lancet*. 2022;399(10325):629-55.
 28. Organization WH. WHO. Antimicrobial resistance 2023.
 29. Samal K, Mahapatra S, Ali MH. Pharmaceutical wastewater as Emerging Contaminants (EC): Treatment technologies, impact on environment and human health. *Energy Nexus*. 2022;6:100076.
 30. Zeng H, Li J, Zhao W, Xu J, Xu H, Li D, et al. The current status and prevention of antibiotic pollution in groundwater in China. *International Journal of Environmental Research and Public Health*. 2022;19(18):11256.
 31. Livermore DM. Tigecycline: what is it, and where should it be used? *Journal of Antimicrobial Chemotherapy*. 2005;56(4):611-4.
 32. Sharma R, Kaur M, Kaur R, Sharma VL, Sobti RC. Exploration on different animal models used in drug-induced adverse reactions research; current scenario and further prospectives. *Advances in Animal Experimentation and Modeling*: Elsevier; 2022. p. 179-93.
 33. Chopra I, Roberts M. Tetracycline antibiotics: mode of action, applications,

- molecular biology, and epidemiology of bacterial resistance. *Microbiology and molecular biology reviews*. 2001;65(2):232-60.
34. Nelson ML, Levy SB. The history of the tetracyclines. *Annals of the New York Academy of Sciences*. 2011;1241(1):17-32.
 35. Liu F, Myers AG. Development of a platform for the discovery and practical synthesis of new tetracycline antibiotics. *Current Opinion in Chemical Biology*. 2016;32:48-57.
 36. Eisen DP. Tetracycline. *Kucers' the use of antibiotics: CRC Press; 2017*. p. 1195-203.
 37. Chukwudi CU. rRNA binding sites and the molecular mechanism of action of the tetracyclines. *Antimicrobial agents and chemotherapy*. 2016;60(8):4433-41.
 38. Tariq S, Rizvi SFA, Anwar U. Tetracycline: classification, structure activity relationship and mechanism of action as a theranostic agent for infectious lesions-a mini review. *Biomed J Sci Tech Res*. 2018;7:5787-96.
 39. Daghrrir R, Drogui P. Tetracycline antibiotics in the environment: a review. *Environmental chemistry letters*. 2013;11:209-27.
 40. Tetracycline: PubChem; 2023.
 41. Leichtweis J, Vieira Y, Welter N, Silvestri S, Dotto GL, Carissimi E. A review of the occurrence, disposal, determination, toxicity and remediation technologies of the tetracycline antibiotic. *Process Safety and Environmental Protection*. 2022;160:25-40.
 42. Amangelsin Y, Semenova Y, Dadar M, Aljofan M, Bjørklund G. The impact of tetracycline pollution on the aquatic environment and removal strategies. *Antibiotics*. 2023;12(3):440.
 43. Ahmad F, Zhu D, Sun J. Environmental fate of tetracycline antibiotics: degradation pathway mechanisms, challenges, and perspectives. *Environmental Sciences Europe*. 2021;33(1):64.

44. Wang F, Wang Z, Zhao Y, Zhang J. Performance of Traditional and Emerging Water-Treatment Technologies in the Removal of Tetracycline Antibiotics. *Catalysts*. 2024;14(4):269.
45. Cevallos-Mendoza J, Amorim CG, Rodríguez-Díaz JM, Montenegro MdCB. Removal of contaminants from water by membrane filtration: a review. *Membranes*. 2022;12(6):570.
46. Rahaman T, Hossain MI, Mousumi Akter S. Advanced Filtration Techniques in Environmental Engineering. Rahaman, T Hossain, MI, Sathi, MA *Advanced Filtration Techniques in Environmental Engineering American Journal of Science and Learning for Development*. 2024;3(2):22-32.
47. Kucera J. *Reverse osmosis*: John Wiley & Sons; 2023.
48. Greenlee LF, Lawler DF, Freeman BD, Marrot B, Moulin P. Reverse osmosis desalination: water sources, technology, and today's challenges. *Water research*. 2009;43(9):2317-48.
49. Grassi M, Kaykioglu G, Belgiorno V, Lofrano G. Removal of emerging contaminants from water and wastewater by adsorption process. *Emerging compounds removal from wastewater: natural and solar based treatments*. 2012:15-37.
50. Rashed MN. Adsorption technique for the removal of organic pollutants from water and wastewater. *Organic pollutants-monitoring, risk and treatment*. 2013;7:167-94.
51. John MM, Benettayeb A, Belkacem M, Mitchel CR, Brahim MH, Benettayeb I, et al. An overview on the key advantages and limitations of batch and dynamic modes of biosorption of metal ions. *Chemosphere*. 2024:142051.
52. Salgado BC, Cardeal RA, Valentini A. Photocatalysis and photodegradation of pollutants. *Nanomaterials Applications for Environmental Matrices*: Elsevier; 2019. p. 449-88.
53. Sadeghfar F, Zalipour Z, Taghizadeh M, Taghizadeh A, Ghaedi M. Photodegradation processes. *Interface Science and Technology*. 32: Elsevier; 2021.

p. 55-124.

54. Kathi S, Mahmoud AED. Trends in Effective Removal of Emerging Contaminants from Wastewater: A Comprehensive Review. *Desalination and Water Treatment*. 2024;100258.
55. Cuerda-Correa EM, Alexandre-Franco MF, Fernández-González C. Advanced oxidation processes for the removal of antibiotics from water. An overview. *Water*. 2019;12(1):102.
56. Toth J. *Adsorption*: CRC Press; 2002.
57. Aljamali NM, Khdur R, Alfatlawi IO. Physical and chemical adsorption and its applications. *International Journal of Thermodynamics and Chemical Kinetics*. 2021;7(2):1-8.
58. Dąbrowski A. Adsorption—from theory to practice. *Advances in colloid and interface science*. 2001;93(1-3):135-224.
59. Alaqarbeh M. Adsorption phenomena: definition, mechanisms, and adsorption types: short review. *RHAZES: Green and Applied Chemistry*. 2021;13:43-51.
60. Ponc V, Knor Z, Cerny S. *Adsorption on solids*: Butterworth; 2018.
61. Rouquerol J, Rouquerol F, Llewellyn P, Maurin G, Sing K. *Adsorption by powders and porous solids: principles, methodology and applications*: Academic press; 2013.
62. Iwuozor KO, Ighalo JO, Emenike EC, Igwegbe CA, Adeniyi AG. Do adsorbent pore size and specific surface area affect the kinetics of methyl orange aqueous phase adsorption? *Journal of Chemistry Letters*. 2021;2(4):188-98.
63. Sadegh H, Ali GA. Potential applications of nanomaterials in wastewater treatment: nanoadsorbents performance. *Advanced treatment techniques for industrial wastewater*: IGI Global; 2019. p. 51-61.
64. Tony MA. Low-cost adsorbents for environmental pollution control: a concise systematic review from the prospective of principles, mechanism and their applications. *Journal of Dispersion Science and Technology*. 2022;43(11):1612-33.

65. Satyam S, Patra S. Innovations and challenges in adsorption-based wastewater remediation: a comprehensive review. *Heliyon*. 2024.
66. Rápó E, Tonk S. Factors affecting synthetic dye adsorption; desorption studies: a review of results from the last five years (2017–2021). *Molecules*. 2021;26(17):5419.
67. Khalaf S, Al-Mahmoud S. Adsorption of tetracycline antibiotic from aqueous solutions using natural Iraqi bentonite. *Egypt J Chem*. 2021; 64 (10): 5511–9.
68. Essington M, Lee J, Seo Y. Adsorption of antibiotics by montmorillonite and kaolinite. *Soil Science Society of America Journal*. 2010;74(5):1577-88.
69. Zhang D, Yin J, Zhao J, Zhu H, Wang C. Adsorption and removal of tetracycline from water by petroleum coke-derived highly porous activated carbon. *Journal of Environmental Chemical Engineering*. 2015;3(3):1504-12.
70. Ji L, Chen W, Duan L, Zhu D. Mechanisms for strong adsorption of tetracycline to carbon nanotubes: a comparative study using activated carbon and graphite as adsorbents. *Environmental science & technology*. 2009;43(7):2322-7.
71. Gao Y, Li Y, Zhang L, Huang H, Hu J, Shah SM, et al. Adsorption and removal of tetracycline antibiotics from aqueous solution by graphene oxide. *Journal of colloid and interface science*. 2012;368(1):540-6.
72. Rautureau M, Figueiredo Gomes CdS, Liewig N, Katouzian-Safadi M, Rautureau M, Figueiredo Gomes CdS, et al. Clay and clay mineral definition. *Clays and Health: Properties and Therapeutic Uses*. 2017:5-31.
73. Bergaya F, Lagaly G. General introduction: clays, clay minerals, and clay science. *Developments in clay science*. 2006;1:1-18.
74. Fuertes V, Reinoso J, Fernández J, Enríquez E. Engineered feldspar-based ceramics: A review of their potential in ceramic industry. *Journal of the European Ceramic Society*. 2022;42(2):307-26.
75. Kumari N, Mohan C. Basics of clay minerals and their characteristic properties. *Clay Clay Miner*. 2021;24(1).

76. Khan S, Ajmal S, Hussain T, Rahman MU. Clay-based materials for enhanced water treatment: adsorption mechanisms, challenges, and future directions. *Journal of Umm Al-Qura University for Applied Sciences*. 2023;1-16.
77. Bakhshi M, Mozdianfard M-R, Hayati-Ashtiani M. Investigating mineralogical and physio-chemical properties of bentonite for water-based fluids. *Kufa Journal of Engineering*. 2020;11(1):79-89.
78. Barton C. Clay minerals. In: Rattan Lal, comp, ed *Encyclopedia of Soil Science* New York, New York: Marcel Dekker: 187-192. 2002.
79. Marchuk S. *The Dynamics of Potassium in some Australian soils* 2016.
80. Oleiwi HB. *Treatment and reuse of produced water from Al-ahdab Iraqi oilfields*. University of Baghdad. 2014.
81. Lagaly G, Ogawa M, Dékány I. Clay mineral organic interactions. *Developments in Clay Science*. 2006;1:309-77.
82. Ross CS, Shannon EV. The minerals of bentonite and related clays and their physical properties 1. *Journal of the American Ceramic Society*. 1926;9(2):77-96.
83. Riess G, Schauburger J. Chemical/physical preprocessing of nanoclay particles. *Polymer Nanoclay Composites: Elsevier*; 2015. p. 27-51.
84. Anderson RL, Ratcliffe I, Greenwell H, Williams P, Cliffe S, Coveney PV. Clay swelling—a challenge in the oilfield. *Earth-Science Reviews*. 2010;98(3-4):201-16.
85. Murray HH. Bentonite applications. *Developments in Clay Science*. 2006;2:111-30.
86. Muhammad N, Siddiqua S. Calcium bentonite vs sodium bentonite: The potential of calcium bentonite for soil foundation. *Materials Today: Proceedings*. 2022;48:822-7.
87. Dhar AK, Himu HA, Bhattacharjee M, Mostufa MG, Parvin F. Insights on applications of bentonite clays for the removal of dyes and heavy metals from wastewater: a review. *Environmental Science and Pollution Research*. 2023;30(3):5440-74.

88. Lin MJ, Song M, Shen XY. Photocatalyst TiO₂ supported on bentonite for water organic pollutants purification: A literature review. *Advanced Materials Research*. 2012;463:967-74.
89. Sreekala SV, Vayalveetil A, Kochu JK, Ramakrishnan RT, Pillai HPS. Bentonite-titanium dioxide functional nanocomposites suitable for wastewater treatment: An integrated photocatalyst-adsorbent system. *New Journal of Chemistry*. 2022;46(10):4772-83.
90. Khan I, Saeed K, Ali N, Khan I, Zhang B, Sadiq M. Heterogeneous photodegradation of industrial dyes: An insight to different mechanisms and rate affecting parameters. *Journal of environmental chemical engineering*. 2020;8(5):104364.
91. Azhar M. Historical overview and future prospects of photocatalysis. *Graphene-Based Photocatalysts: From Fundamentals to Applications*: Springer; 2024. p. 47-65.
92. Ameta R, Solanki MS, Benjamin S, Ameta SC. *Photocatalysis. Advanced oxidation processes for waste water treatment*: Elsevier; 2018. p. 135-75.
93. Parmon V, Emeline A, Serpone N. Glossary of terms in photocatalysis and radiocatalysis. *International Journal of photoenergy*. 2002;4:91-131.
94. Belver C, Bedia J, Gómez-Avilés A, Peñas-Garzón M, Rodríguez JJ. Semiconductor photocatalysis for water purification. *Nanoscale materials in water purification*: Elsevier; 2019. p. 581-651.
95. Ge J, Zhang Y, Heo Y-J, Park S-J. Advanced design and synthesis of composite photocatalysts for the remediation of wastewater: A review. *Catalysts*. 2019;9(2):122.
96. Kołodziejczak-Radzimska A, Jesionowski T. Zinc oxide—from synthesis to application: a review. *Materials*. 2014;7(4):2833-81.
97. Vyas S. A short review on properties and applications of zinc oxide based thin films and devices: ZnO as a promising material for applications in electronics,

- optoelectronics, biomedical and sensors. Johnson Matthey Technology Review. 2020;64(2):202-18.
98. Mayhew KW. New thermodynamics: Rethinking the Science of climate change. European Journal of Engineering and Technology Research. 2020;5(5):559-64.
99. Siva N, Sakthi D, Ragupathy S, Arun V, Kannadasan N. Synthesis, structural, optical and photocatalytic behavior of Sn doped ZnO nanoparticles. Materials Science and Engineering: B. 2020;253:114497.
100. Zyoud AH, Asaad S, Zyoud SH, Zyoud SH, Helal MH, Qamhieh N, et al. Raw clay supported ZnO nanoparticles in photodegradation of 2-chlorophenol under direct solar radiations. Journal of Environmental Chemical Engineering. 2020;8(5):104227.
101. Patterson A. The Scherrer formula for X-ray particle size determination. Physical review. 1939;56(10):978.
102. Jauncey G. The scattering of x-rays and Bragg's law. Proceedings of the national academy of sciences. 1924;10(2):57-60.
103. Zyoud AH, Zubi A, Zyoud SH, Hilal MH, Zyoud S, Qamhieh N, et al. Kaolin-supported ZnO nanoparticle catalysts in self-sensitized tetracycline photodegradation: zero-point charge and pH effects. Applied Clay Science. 2019;182:105294.
104. Dedic M, Gutic S, Gicevic A, Becic E, Imamovic B, Markovic D, et al. Application of membrane filters in determination of the adsorption of tetracycline hydrochloride on graphene oxide. Pharmacia. 2020;67:339-45.
105. Chang P-H, Li Z, Jean J-S, Jiang W-T, Wang C-J, Lin K-H. Adsorption of tetracycline on 2: 1 layered non-swelling clay mineral illite. Applied Clay Science. 2012;67:158-63.
106. Li Z, Schulz L, Ackley C, Fenske N. Adsorption of tetracycline on kaolinite with pH-dependent surface charges. Journal of colloid and interface science. 2010;351(1):254-60.

107. Zyoud A, Zorba T, Helal M, Zyoud S, Qamhiya N, Hajamohideen A, et al. Direct sunlight-driven degradation of 2-chlorophenol catalyzed by kaolinite-supported ZnO. *International Journal of Environmental Science and Technology*. 2019;16:6267-76.
108. Peleg M, Normand MD, Corradini MG. The Arrhenius equation revisited. *Critical reviews in food science and nutrition*. 2012;52(9):830-51.
109. Lasaga AC. Rate laws of chemical reactions. *Rev Mineral;(United States)*. 1981;8.

Appendices

Appendix A

Figures

Figure A.1

Basic structures of clay minerals: a) Octahedral sheets and b) tetrahedral sheets.

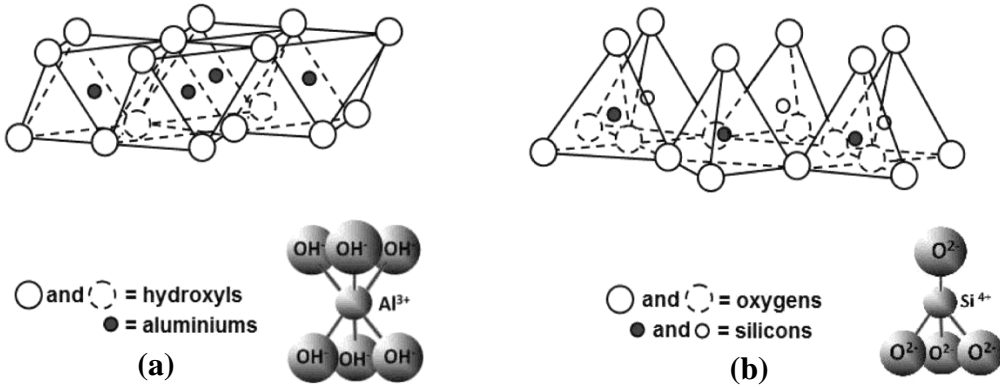


Figure A.2

Structures of a) 1:1 and b) 2:1 clay minerals.

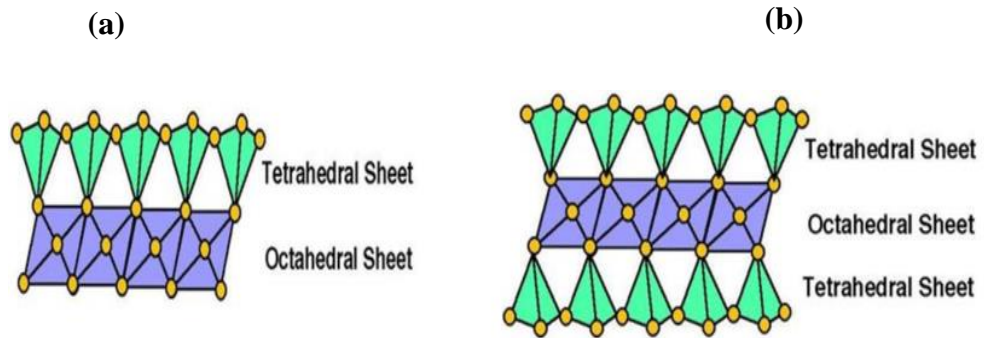


Figure A.3

Structure of expandable and nonexpandable 2:1 clay minerals.

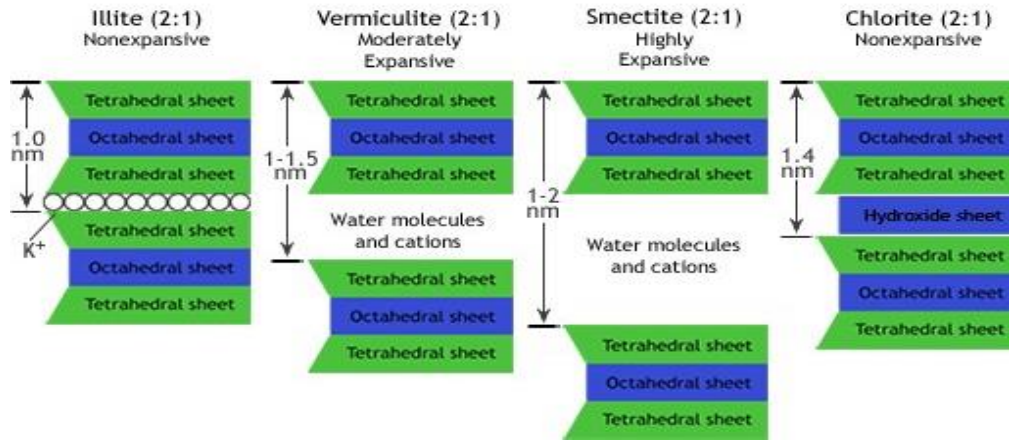


Figure A.4

Basic structure of bentonite clay.

BENTONITE STRUCTURE

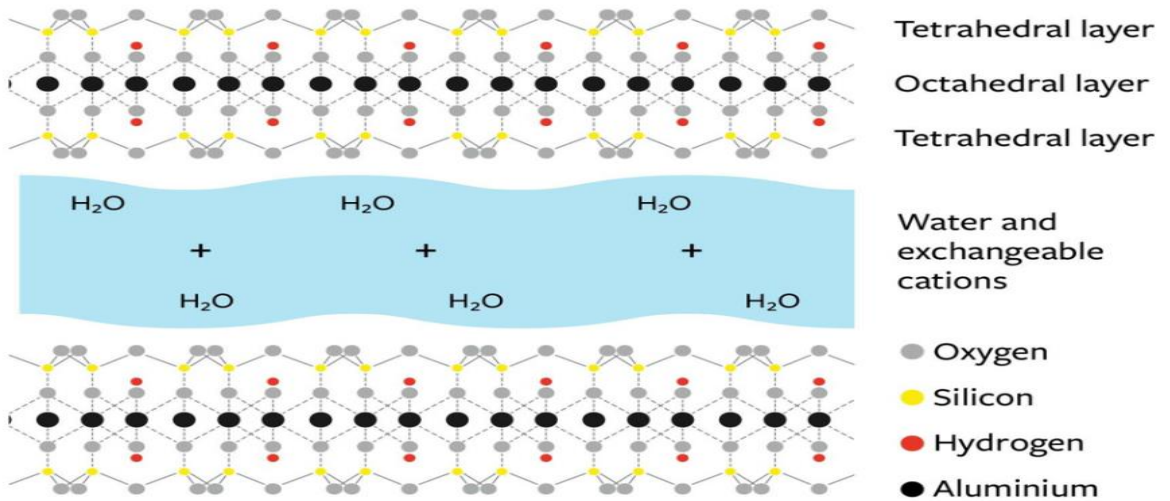


Figure A.5

Absorption spectra of the tetracycline solution in distilled water at neutral pH at room temperature.

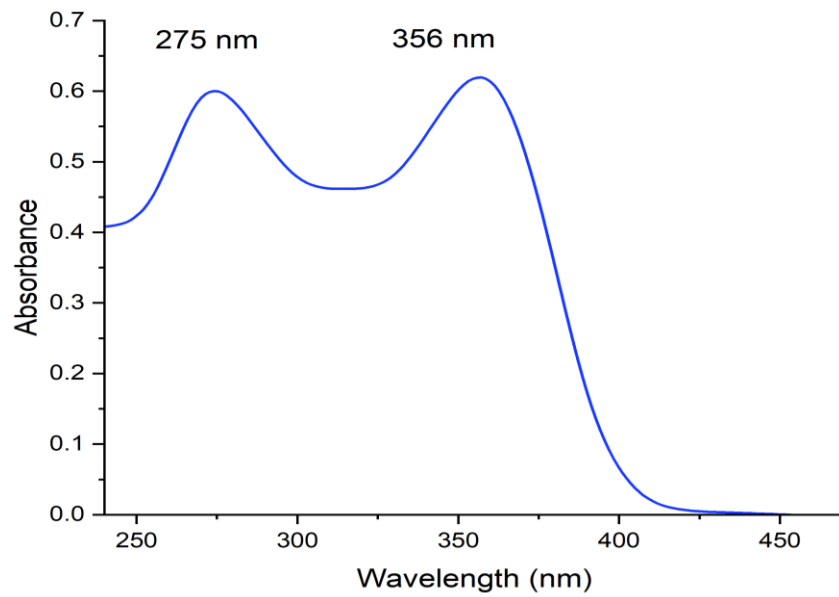


Figure A.6

Absorption spectra of the photodegradation of tetracycline in the presence of a ZnO/bentonite photocatalyst. The experiment was performed using a tetracycline solution (100 ml, 40 ppm) at 25 °C and basic pH medium with 0.1 g of ZnO/bentonite under simulated solar light.

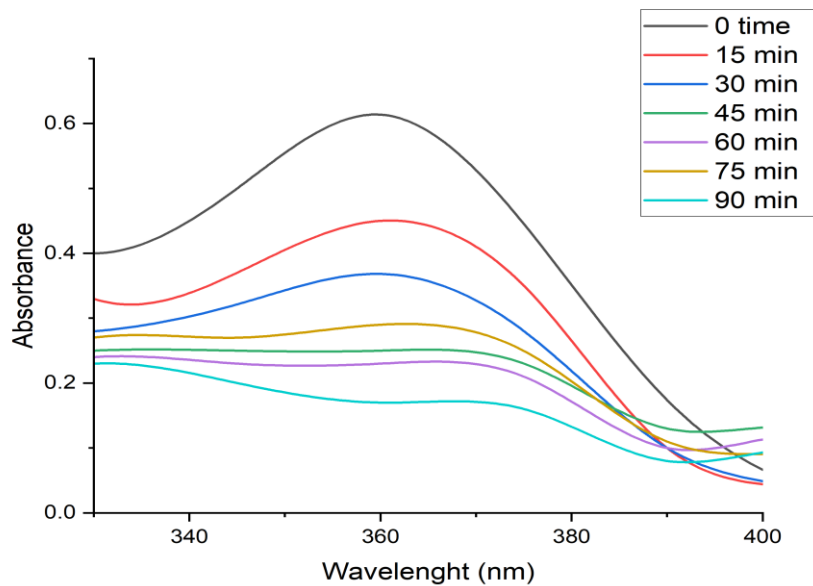


Figure A.7

Effects of light on tetracycline removal: Comparison of the photodegradation reactions of tetracycline alone and with three different catalysts (ZnO, bentonite, and ZnO/bentonite) over time (initial concentration of 40 ppm, temperature of 25 °C and 0.1 g of each catalyst).

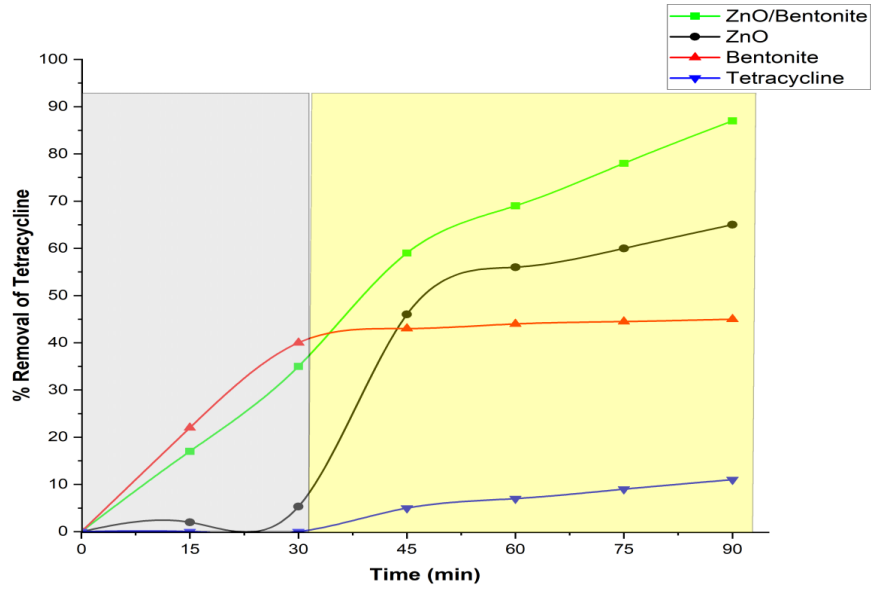


Figure A.8

Effects of the absence of light on tetracycline removal: Comparison of the effects of three different catalysts (ZnO, bentonite, and ZnO/bentonite) on the photodegradation of tetracycline with time (initial concentration of 40 ppm, temperature of 25 °C and 0.1 g of each catalyst).

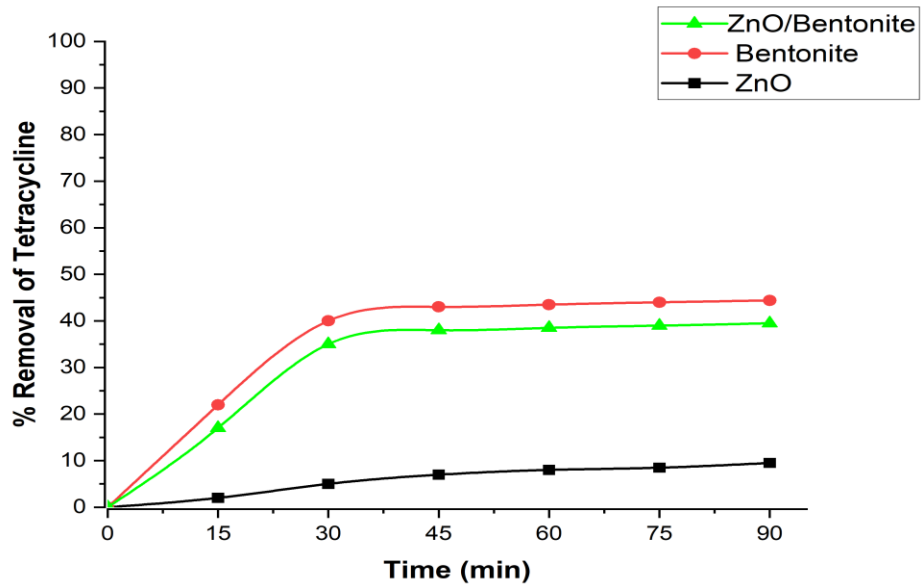


Figure A.9

The chemical structure of a tetracycline molecule, with pK_a values for the main functional groups: $pK_{a1} = 3.3$, $pK_{a2} = 7.7$, and $pK_{a3} = 9.7$, indicating the dissociation and ionization points of the compound when the pH changes.

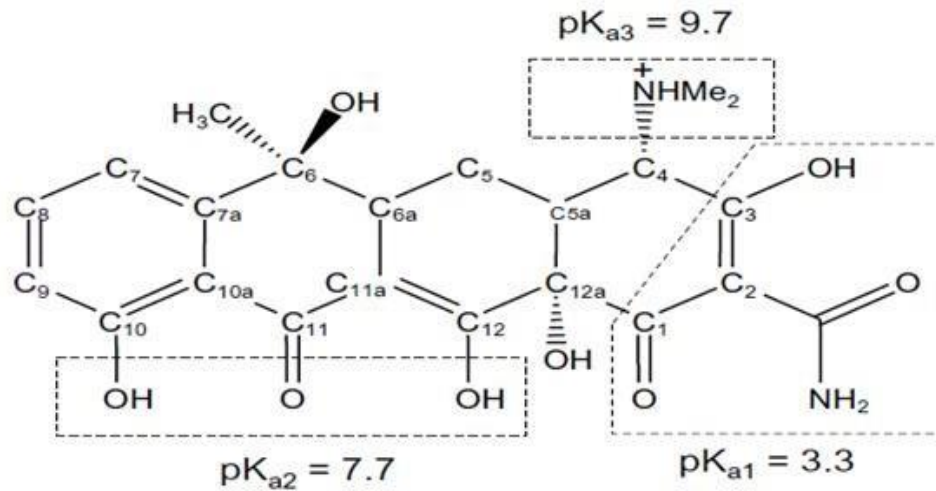


Figure A.10

Different ionic forms of tetracycline (TCH_3^+ , TCH_2^+ , TCH^- , TC^{2-}) at different pH values

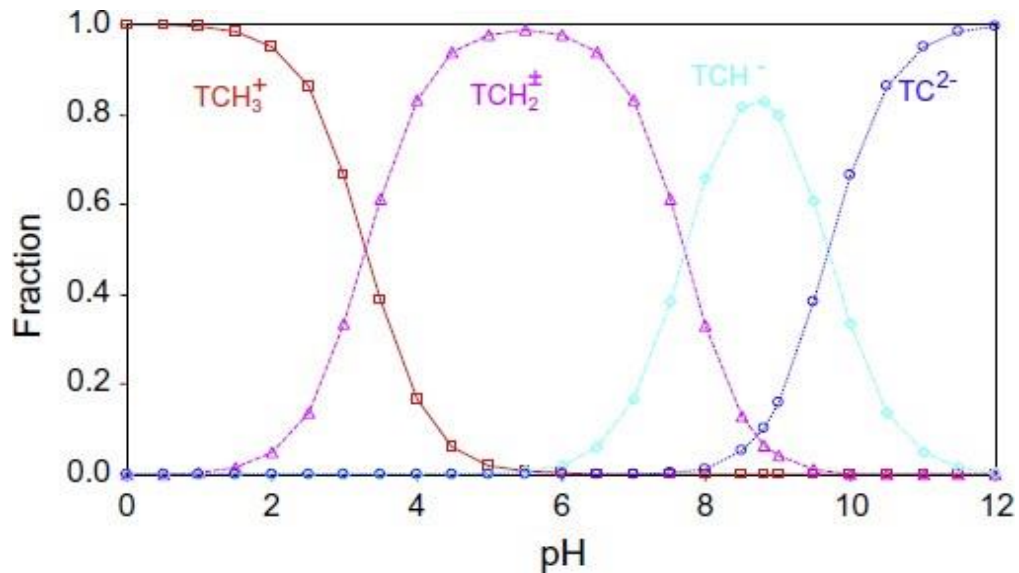


Figure A.11

Effect of different pH values (3.0, 5.3, 7.0, 8.5, 10.1) on the percentage of tetracycline removal of tetracycline over time, with initial concentration of 40 ppm, temperature set at 25°C, and 0.1 g of ZnO/bentonite catalyst.

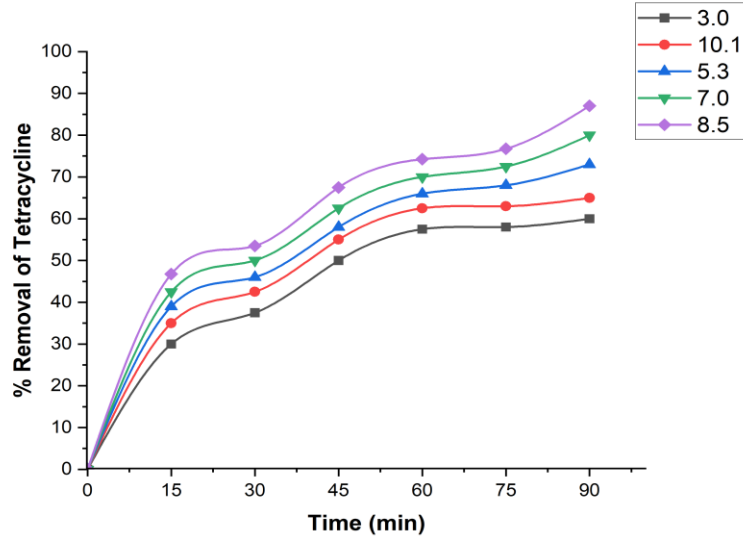


Figure A.12

Effect of different temperatures values (7°C, 15°C, 30°C, 57°C) on the percentage of tetracycline removal of tetracycline over time, with initial concentration of 40 ppm, basic pH medium, and 0.1 g of ZnO/bentonite catalyst.

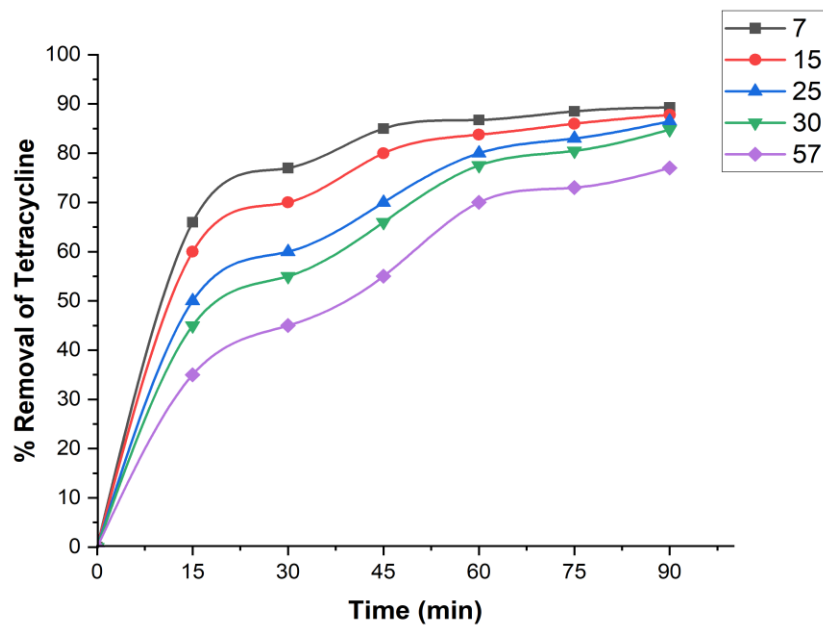


Figure A.13

Effect of different catalyst amounts (0.05 g, 0.1 g, 0.2 g, 0.3 g, 0.4 g, 0.5 g) on the percentage of tetracycline removal over time, with an initial concentration of 40 ppm, basic pH medium, and temperature set at 25°C.

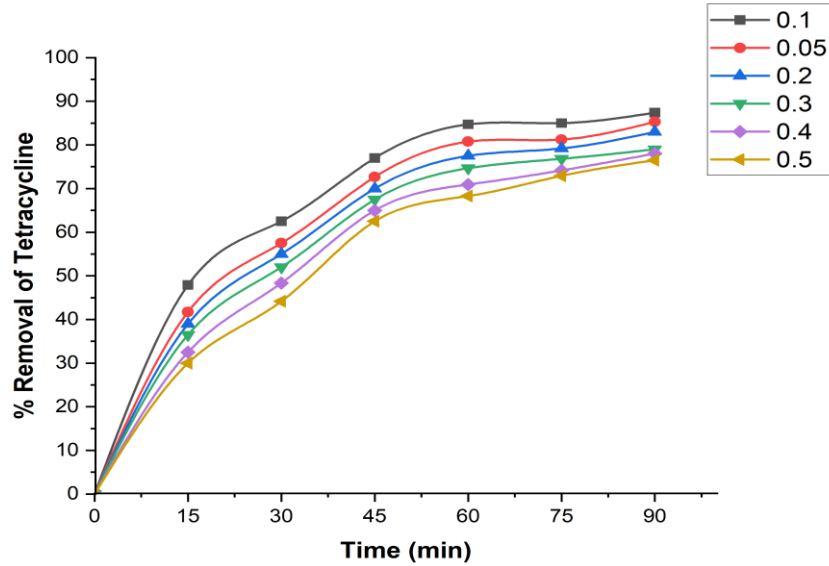


Figure A.14

Effects of different tetracycline concentrations (10 ppm, 20 ppm, 30 ppm, 40 ppm, and 50 ppm) on the percentage and amount of tetracycline removed over time, with 0.1 g of ZnO/bentonite catalyst, basic pH medium, and temperature set at 25 °C. The red curve represents the percentage removal of tetracycline (left y-axis), whereas the blue curve represents the amount of tetracycline removed in mg/L (right y-axis).

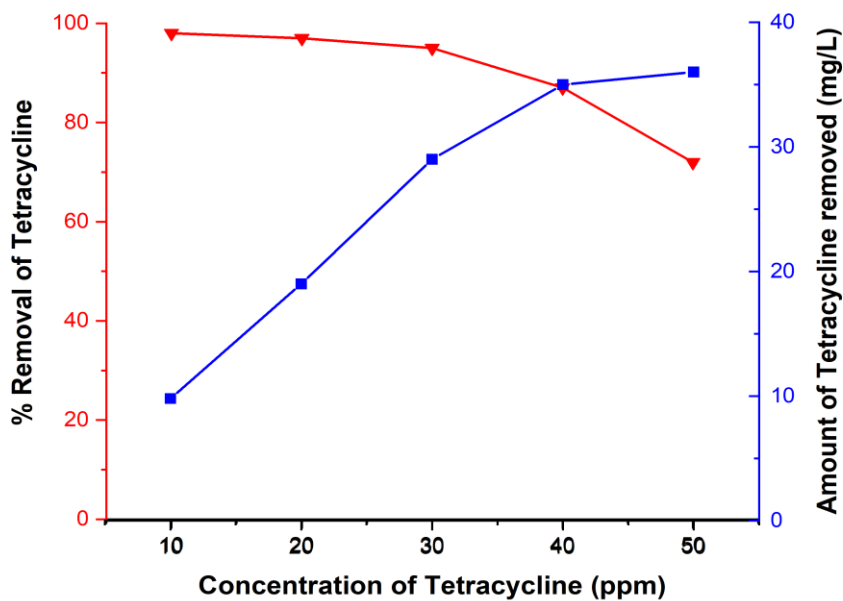


Figure A.15

Effect of oxygen on the percentage of tetracycline removal over time, with an initial concentration of 40 ppm, 0.1 g of ZnO/bentonite catalyst, basic pH medium, and temperature set at 25 °C.

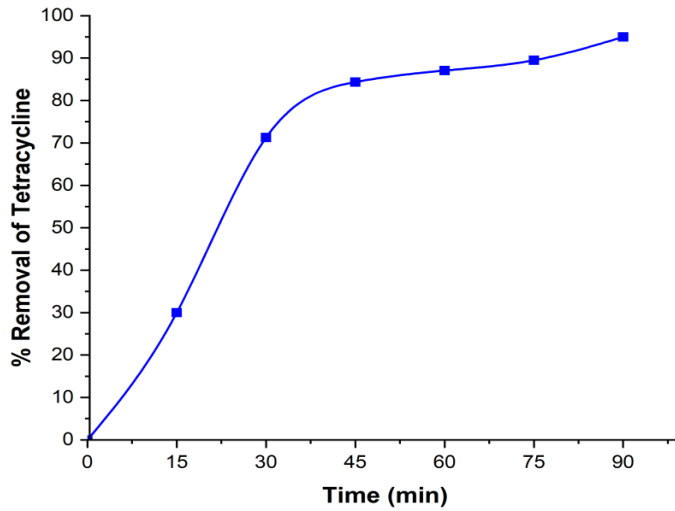


Figure A.16

Effect of carbon dioxide on the percentage of tetracycline removal over time, with an initial concentration of 40 ppm, 0.1 g of ZnO/bentonite catalyst, basic pH medium, and temperature set at 25 °C.

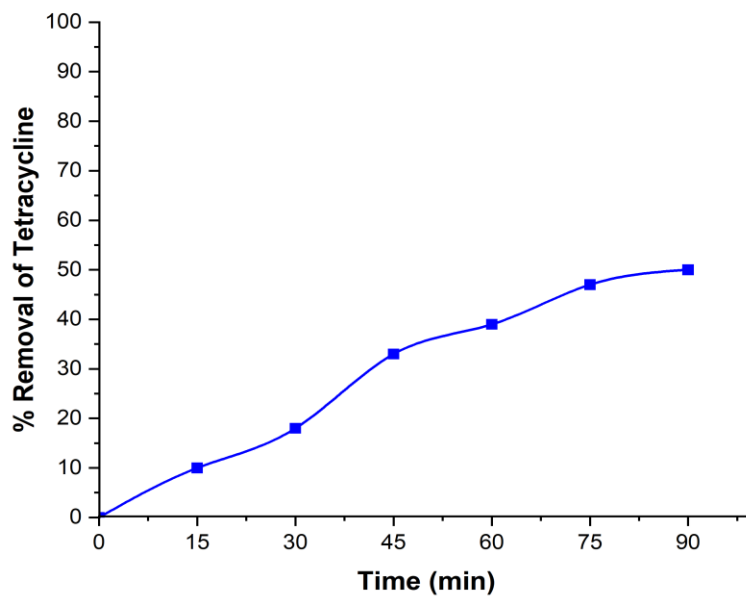


Figure A.17

Relationship between $\ln(k)$ and $\frac{1}{T}$ in the tetracycline removal reaction using the ZnO/bentonite catalyst, where the data follow a straight line with the regression equation ($y = -602.84x + 6.1598$).

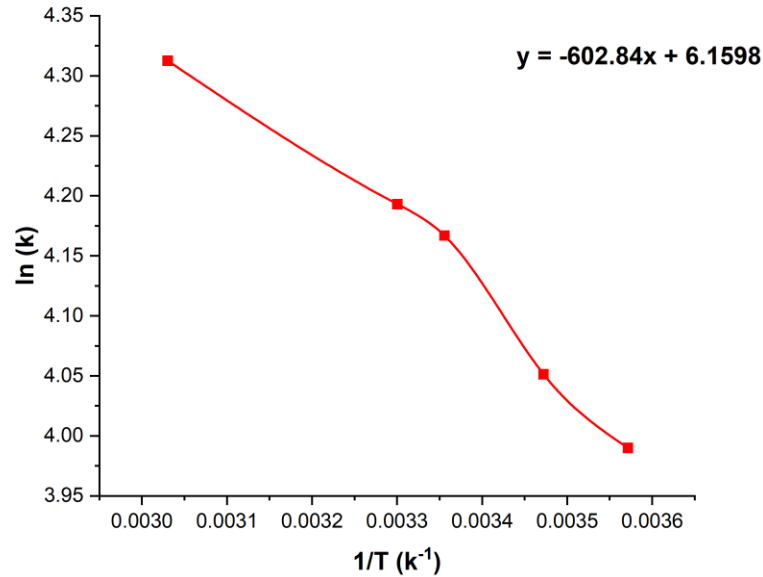


Figure A.18

Relationship between $\ln(\text{rate})$ and $\ln([\text{tetracycline concentration}])$, with the straight-line equation $y = 0.21497x + 4.66428$ and a correlation coefficient $R^2 = 0.93135$.

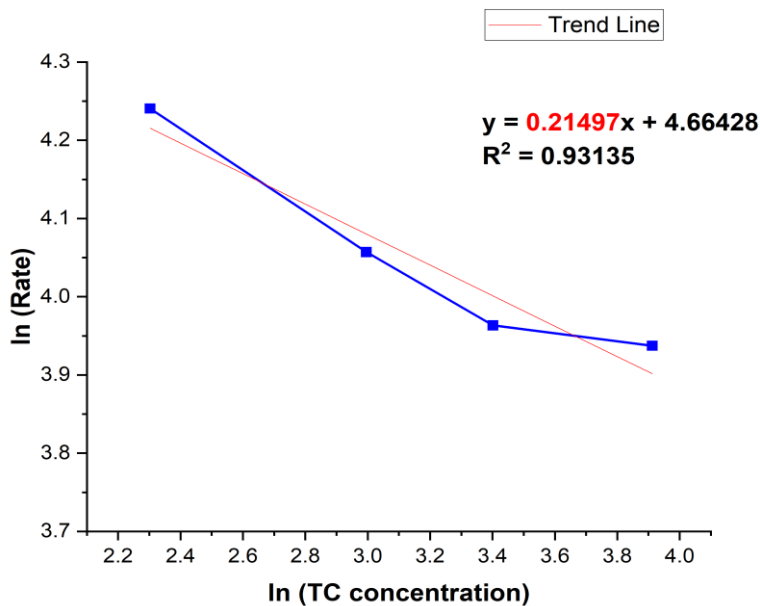


Figure A.19

Relationship between $\ln(\text{Rate})$ and $\ln([\text{catalyst amount}])$, with the straight-line equation $y = 0.10224x + 4.1696$ and a correlation coefficient $R^2 = 0.91324$.

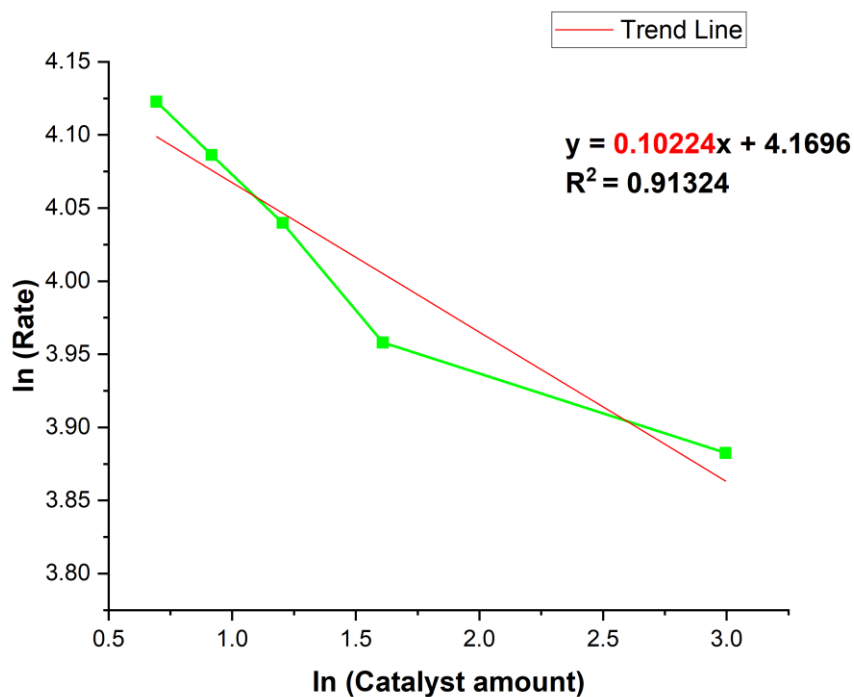


Figure A.20

Photocatalytic efficiency of ZnO/bentonite after recovery and reuse. Experiments were performed using a tetracycline solution (100 mL, 40 ppm) with 0.1 g of catalyst at a temperature of 25 °C and pH 8.5.

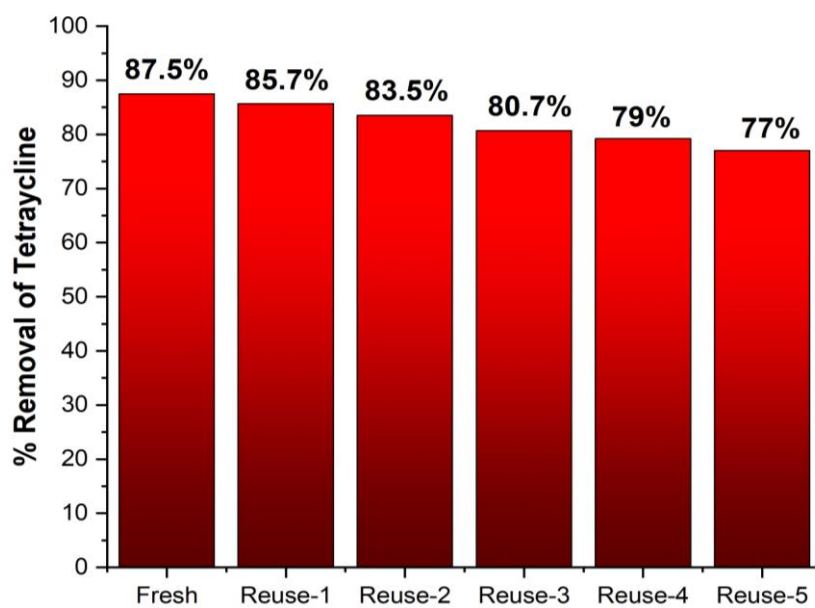


Figure A.21

Electronic absorption spectral confirmation of complete mineralization of tetracycline by photodegradation with time. The reaction was conducted with TC (100.0 mL, 40 ppm) and 0.1 g of ZnO/bentonite at pH ~8.5 at 25 °C.

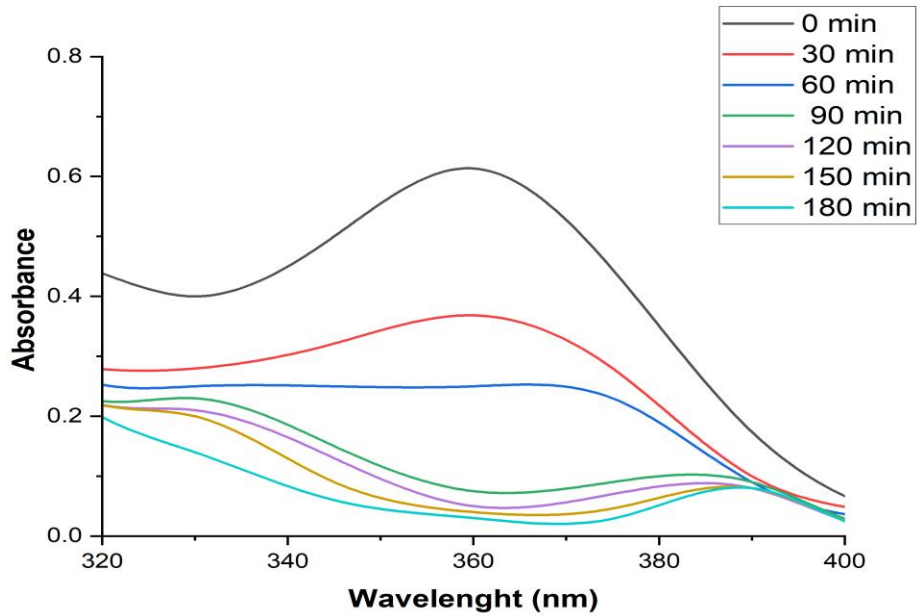


Figure A.22

FT-IR spectra of tetracycline, with air utilized as the blank.

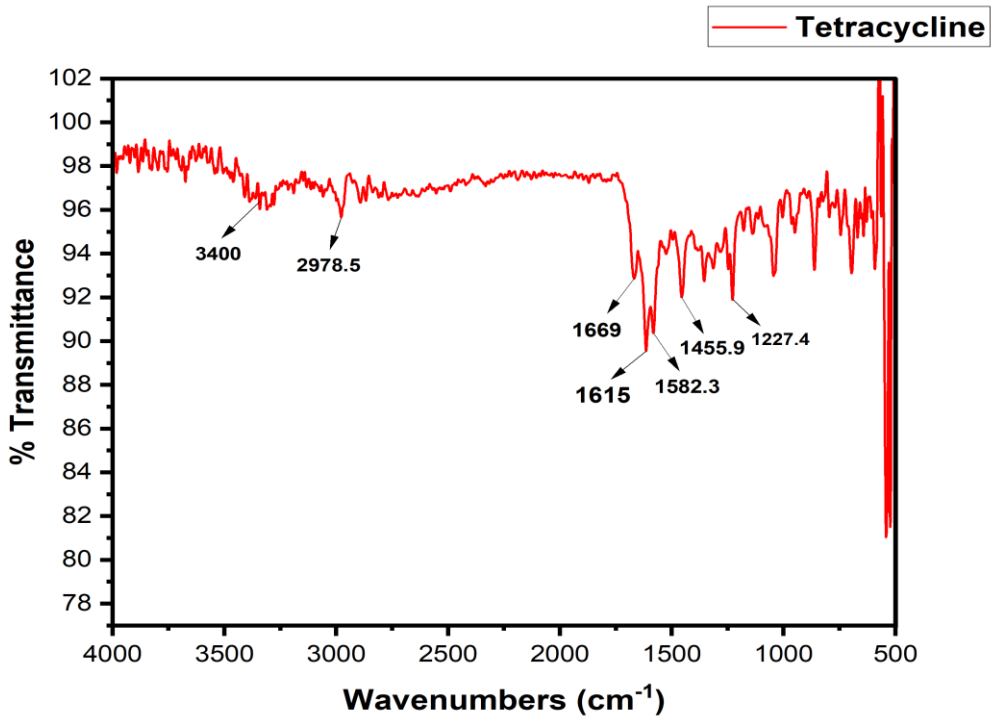


Figure A.23

FT-IR spectra of the ZnO/bentonite catalyst, with air utilized as the blank.

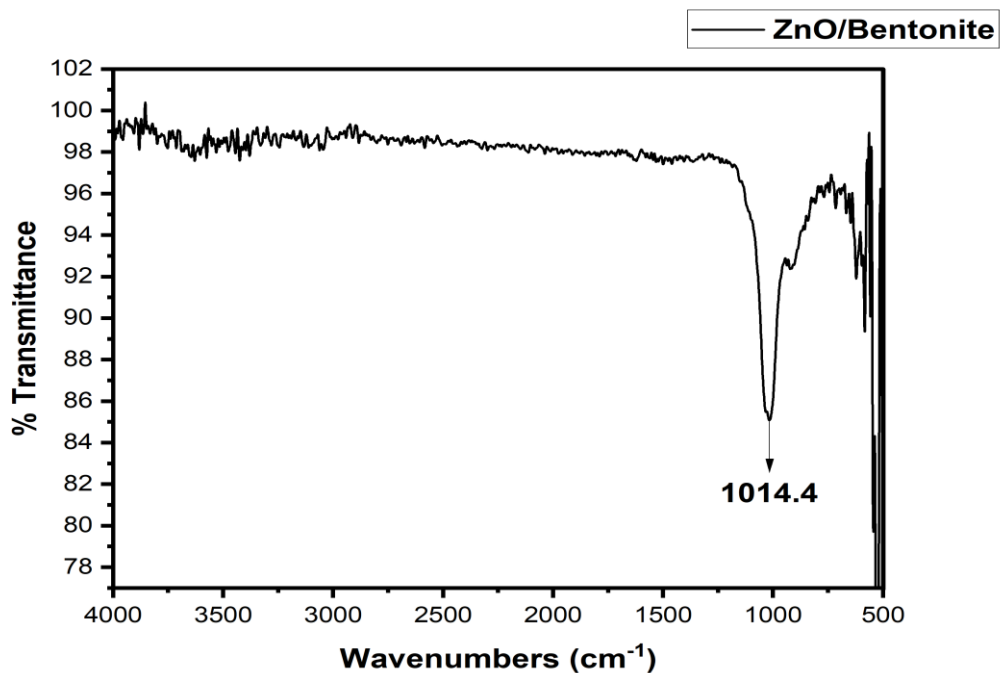


Figure A.24

FT-IR spectra of tetracycline on the catalyst surface after 30 min of photodegradation. The reaction was performed with TC (100.0 mL, 40 ppm) and 0.1 g of ZnO/bentonite at pH ~8.5 at 25 °C. Air was used as the blank.

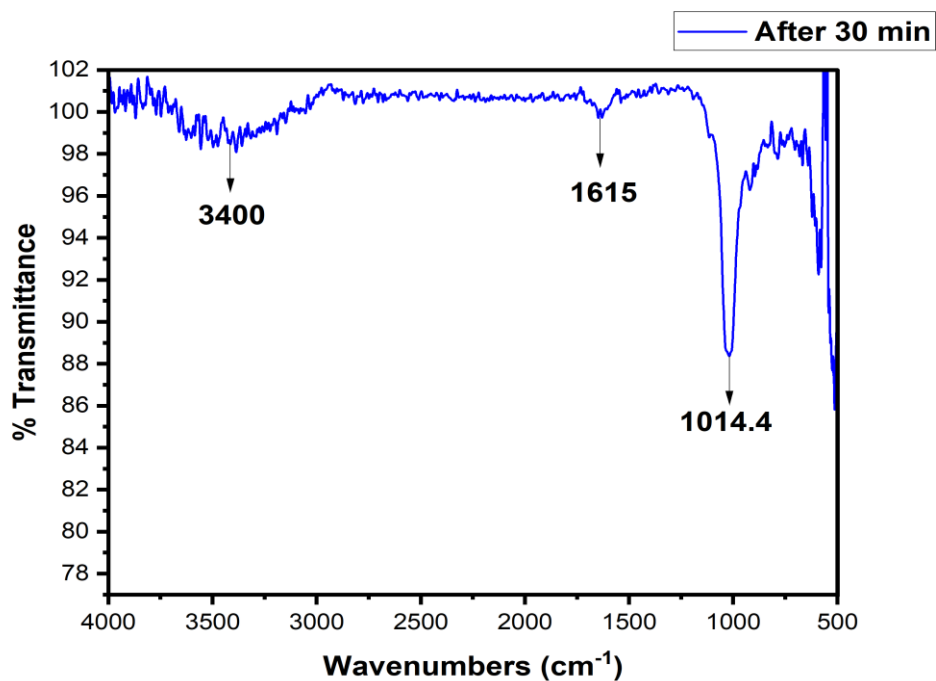


Figure A.25

FT-IR spectra of tetracycline on the catalyst surface after 90 min of photodegradation. The reaction was performed with TC (100.0 mL, 40 ppm) and 0.1 g of ZnO/bentonite at pH ~8.5 at 25 °C. Air was used as the blank.

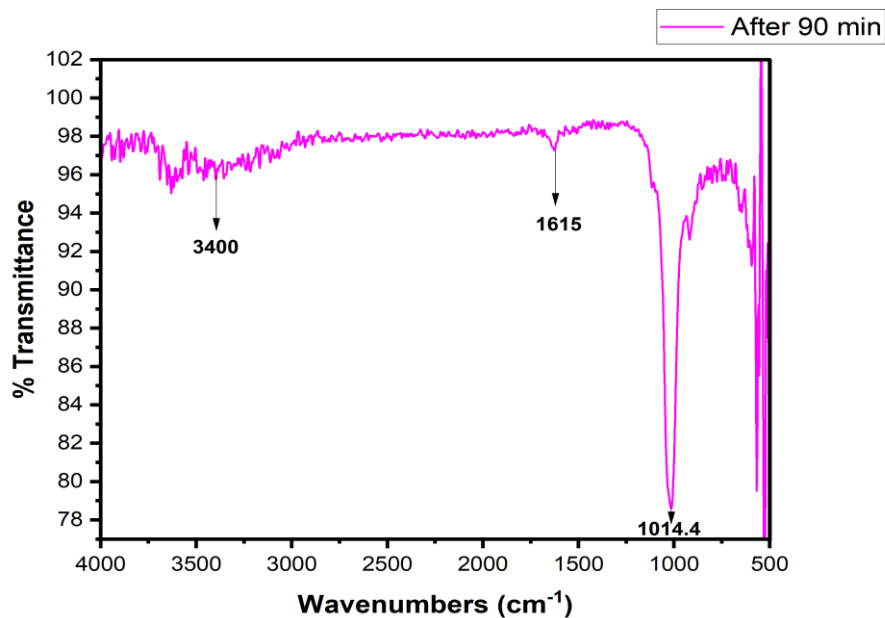
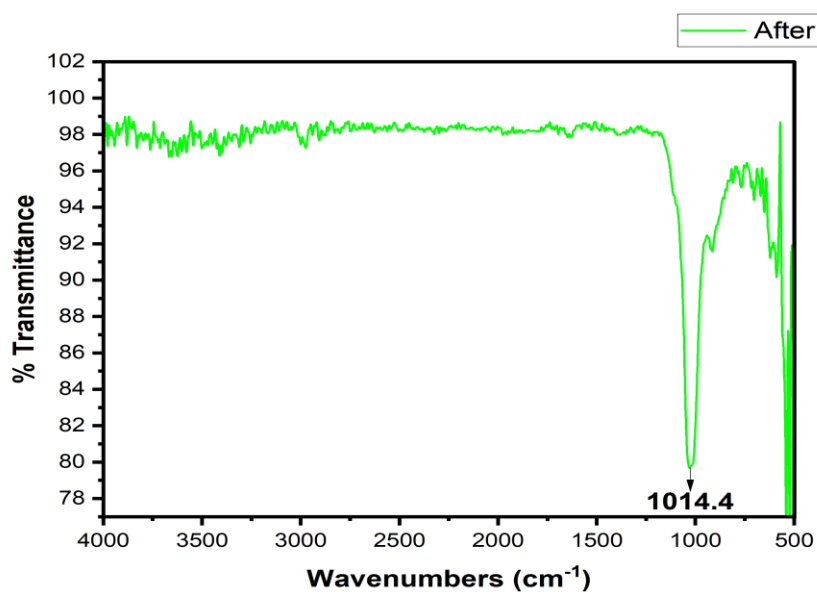


Figure A.26

FT-IR spectra of tetracycline on the catalyst surface after 180 min of photodegradation. The reaction was performed with TC (100.0 mL, 40 ppm) and 0.1 g of ZnO/bentonite at pH ~8.5 at 25 °C. Air was used as the blank.





جامعة النجاح الوطنية
كلية الدراسات العليا

استخدام مترابك أكسيد الزنك/البنطونيت لإزالة التتراسيكلين من الماء
من خلال الامتزاز والتحلل الضوئي

إعداد

ياسمين علاء محمد حمدان

إشراف

أ.د. عاهد زيود

قدمت هذه الرسالة استكمالاً لمتطلبات الحصول على درجة الماجستير في الكيمياء، من كلية الدراسات العليا، في
جامعة النجاح الوطنية، نابلس - فلسطين.

2025

استخدام مترابك أكسيد الزنك/البنطونيت لإزالة التتراسيكلين من الماء من خلال الامتزاز والتحلل الضوئي

إعداد
ياسمين علاء محمد حمدان
إشراف
أ.د. عاهد زيود

الملخص

يُعد تلوث المياه بالمستحضرات الصيدلانية، وخاصةً التتراسيكلين، مشكلة بيئية ملحة وسريعة التقاوم، ويتقاوم هذا التلوث نتيجةً لزيادة تعاطي الأدوية والتخلص غير السليم منها. وهذا يُؤكد على الحاجة إلى استراتيجيات وأساليب لمعالجة المياه الملوثة بطريقة تحمي البيئة والكائنات الحية من الآثار السلبية لنفايات التتراسيكلين.

يُظهر مُركب أكسيد الزنك/البنطونيت قدرات امتصاص ممتازة بفضل البنية المسامية لطين البنطونيت، التي تُوفر مساحة سطح كبيرة مثالية لجذب جزيئات الملوثات والتقاطها. من ناحية أخرى، يُظهر المُركب كفاءة ملحوظة في تحليل هذه الملوثات بالاستفادة من خصائص أكسيد الزنك التحفيزية الضوئية، حيث يعمل كمُحفز ضوئي عالي الفعالية تحت الأشعة فوق البنفسجية، مما يُساعد في تحلل الملوثات إلى مكونات أقل ضرراً.

في هذه الدراسة، تم دعم أكسيد الزنك على البنطونيت واستخدامه كمُحفز ضوئي تحت ضوء شمسي مُحاكي. شمل البحث دراسة الخصائص الفيزيائية والكيميائية للمركب عبر طرق تحليلية متنوعة. تُشهم هذه الدراسة في فهم بنية هذه المادة وتركيبها، وفهم فعاليتها في معالجة الملوثات. إضافةً إلى ذلك، أُجريت دراسة حركية لتقييم كفاءة إزالة التتراسيكلين وفهم آلية التفاعل.

كما تم تقييم أداء كلٍّ من الامتزاز والتحفيز الضوئي لمركبات أكسيد الزنك/البنطونيت في إزالة التتراسيكلين

من الماء في ظل ظروف مختلفة، مثل الرقم الهيدروجيني، وتركيز التتراسيكلين، ودرجة الحرارة، وكمية المحفز، وعوامل أخرى، مثل تأثيرات غاز الأكسجين وغاز ثاني أكسيد الكربون، حيث حقق المركب معدلات تحلل عالية بكفاءة ملحوظة وصلت إلى 87%. بالإضافة إلى ذلك، تم تحقيق تمعدن شبه كامل بنسبة تصل إلى 98%، مما يؤكد قدرة المحفز على إجراء التحلل الكامل للمضاد الحيوي التتراسيكلين إلى نواتج ثانوية غير سامة. بالإضافة إلى ذلك، يُمكن إعادة استخدام هذا المركب مع الحفاظ على أدائه الجيد، مما يجعله حلاً مستدامًا وفعالاً لمعالجة تلوث المياه وحماية البيئة.

الكلمات المفتاحية: تلوث المياه، التتراسيكلين، مركب أكسيد الزنك/البنطونيت، المحفز الضوئي، الامتزاز، التحفيز الضوئي، التمعدن الكامل.